

**ISTANBUL TECHNICAL UNIVERSITY « INSTITUTE OF SCIENCE AND TECHNOLOGY**

**POLY(VINYLDENE FLUORIDE) BASED COPOLYMERS**

**M. Sc. Thesis by**

**Nergiz BOZOK**

**Department: Polymer Science and Technology**

**Programme: Polymer Science and Technology**

**Supervisor: Prof.Dr. Metin H. ACAR**

**OCTOBER 2008**

**POLY(VINYLLIDENE FLUORIDE) BASED COPOLYMERS**

**M. Sc. Thesis by  
Nergiz BOZOK  
(515061019)**

**Date of submission : 15 September 2008  
Date of Defence Examination : 10 October 2008**

**Supervisor : Prof. Dr. Metin H. ACAR**

**Members of Examining Committee : Prof. Dr. Gürkan HIZAL (I.T.U.)  
Prof. Dr. Yusuf Menciloglu (S.U.)**

**OCTOBER 2008**

**PVDF KÖKENLİ AŞI KOPOLİMERLER**

**YÜKSEK LİSANS TEZİ**  
**Nergiz BOZOK**  
**(515061019)**

**Tezin Enstitüye Verildiği Tarih : 15 Eylül 2008**  
**Tezin Savunulduğu Tarih : 10 Ekim 2008**

**Tez Danışmanı : Prof. Dr. Metin H. ACAR (İ.T.Ü.)**  
**Diğer Jüri Üyeleri : Prof. Dr. Gürkan HIZAL(İ.T.Ü)**  
**Prof. Dr. Yusuf Menciloglu (S.Ü.)**

**EKİM 2008**

## **ACKNOWLEDGEMENT**

This master study has been carried out at Istanbul Technical University, Polymer Science and Technology Department of Institute of Science and Technology.

I would like to express my gratitude to my supervisor Prof. Dr. Metin H. ACAR for his invaluable help, patience and helpful critics throughout in this research.

I would like to thank to Prof. Dr. Yusuf MENCELOGLU for his helpful critics throughout in this research.

I especially thank to my colleagues RA&TA Şebnem İNCEOĞLU, M.Sc. Leyla BAYKAL, and Artun ZORVARYAN for their tolerance and supportive attitudes during my laboratory study.

I would like to thank Burcin YILDIZ at Sabanci University for <sup>1</sup>H-NMR measurements, Burak BIRKAN and Burcu SANER at Sabanci University for thermal analyses measurements.

I am also grateful to my family for their moral support and understanding during all stages involved in the preparation of this research.

SEPTEMBER 2008

Nergiz BOZOK

## TABLE OF CONTENTS

<b>ACKNOWLEDGEMENT</b>	<b>ii</b>
<b>LIST OF ABBREVIATIONS</b>	<b>v</b>
<b>LIST OF TABLES</b>	<b>vii</b>
<b>LIST OF FIGURES</b>	<b>viii</b>
<b>SUMMARY</b>	<b>x</b>
<b>ÖZET</b>	<b>xi</b>
<b>1. INTRODUCTION</b>	<b>1</b>
<b>2. THEORETICAL SECTION</b>	<b>4</b>
2.1. Fluoropolymers	4
2.2. PVDF-Based Graft Copolymers	6
2.2.1. Synthesis of PVDF graft copolymers by ozone activated polymer	8
2.2.1.1. Synthesis of PAA- <i>g</i> -PVDF graft copolymer by radical induced polymerizations	8
2.2.1.2. Synthesis of PVDF- <i>g</i> -PEOMA graft copolymer by ATRP	10
2.2.1.3. Synthesis of PVDF- <i>g</i> -PBIEA- <i>g</i> -NAPSS, PVDF- <i>g</i> -PBIEA- <i>g</i> -PEGMA, PVDF- <i>g</i> -PBIEA- <i>g</i> -PDMAEMA graft copolymers by ATRP	10
2.2.1.4. Synthesis of PVDF- <i>g</i> -PAA- <i>b</i> -PNIPAAM by RAFT	11
2.2.2. Synthesis of PVDF-based graft copolymers by irradiated PVDF	11
2.2.2.1. Synthesis of PVDF - <i>g</i> - PSSA graft copolymer	12
2.2.2.2. Synthesis of PVDF- <i>g</i> -PVBC graft copolymer	13
2.2.2.3. Synthesis of PVDF- <i>g</i> -PMMA graft copolymer	15
2.2.2.4. Synthesis of PVDF- <i>g</i> -PCMS graft copolymer by ATRP	15
2.2.3. Synthesis of PVDF-based graft copolymer by direct initiation of PVDF	15
2.2.3.1. Synthesis of PVDF - <i>g</i> - POEM, PVDF- <i>g</i> -PMMA graft copolymers by ATRP	15
2.2.3.2. Synthesis of PVDF- <i>g</i> -PMMA graft copolymer by ATRP	16
2.2.4. Synthesis of PVDF-based graft copolymer by functionalized PVDF	16
2.3. Free Radical Polymerization	17
2.3.1. Controlled/living radical polymerization	18
2.3.2. Atom transfer radical polymerization	20
2.3.2.1. Monomers	22
2.3.2.2. Initiators	22
2.3.2.3. Ligands	23

2.3.2.4. Transition metal complexes	25
2.3.2.5. Solvents	26
2.3.2.6. Temperature and reaction time	26
2.3.2.7. Kinetics of ATRP	26
2.3.3. Activator generated by electron transfer ATRP	29
2.4. Applications of PVDF-Based Graft Copolymers	30
<b>3. EXPERIMENTAL PART</b>	<b>35</b>
3.1. Chemicals	35
3.2. PVDF-Based Graft Copolymerization by ATRP	38
3.2.1. Synthesis of PVDF- <i>g</i> -PAA graft copolymer	38
3.2.2. Synthesis of PVDF- <i>g</i> -PSPMAP graft copolymer	38
3.2.3. Synthesis of PVDF- <i>g</i> -PSAPMA-TEA graft copolymer	39
3.2.4. Synthesis of PVDF- <i>g</i> -PHEMA graft copolymer	40
3.2.5. Synthesis of PVDF- <i>g</i> -PHEA graft copolymer	40
3.2.6. Synthesis of PVDF- <i>g</i> -PAMPS graft copolymer	41
3.2.7. Synthesis of PVDF- <i>g</i> -PVPA graft copolymer	41
3.2.8. Synthesis of PVDF- <i>g</i> -PGMA graft copolymer	42
3.2.9. Synthesis of PVDF- <i>g</i> -PSA graft copolymer	42
3.3. PVDF Based Graft Copolymerization by AGET-ATRP	44
3.3.1. Synthesis of PVDF- <i>g</i> -PSPMAP graft copolymer	44
3.3.2. Synthesis of PVDF- <i>g</i> -PGMA graft copolymer	44
3.3.3. Synthesis of PVDF- <i>g</i> -PEGMAP graft copolymer	45
3.3.4. Synthesis of PVDF- <i>g</i> -PHEA graft copolymer	46
3.3.5. Synthesis of PVDF- <i>g</i> -PHEMA graft copolymer	46
3.3.6. Synthesis of PVDF- <i>g</i> -PAMPS graft copolymer	47
3.3.7. Synthesis of PVDF- <i>g</i> -PVPA graft copolymer	48
3.4. Characterization	48
<b>4. RESULTS AND DISCUSSION</b>	<b>50</b>
4.1. Synthesis of PVDF-Based Graft Copolymers by ATRP	50
4.2. Synthesis of PVDF-Based Graft Copolymers by AGET-ATRP	65
<b>5. CONCLUSION AND RECOMMENDATIONS</b>	<b>66</b>
<b>REFERENCES</b>	<b>68</b>
<b>AUTOBIOGRAPHY</b>	<b>73</b>

## LIST OF ABBREVIATIONS

<b>ATRP</b>	: Atom Transfer Radical Polymerization
<b>AGET-ATRP</b>	: Activator Generated by Electron Transfer for Atom Transfer Radical Polymerization
<b>PVDF</b>	: Poly(vinylidene fluoride)
<b><i>t</i>BA</b>	: Tertiary Butyl Acrylate
<b>S</b>	: Styrene
<b>HEMA</b>	: 2-Hydroxy Ethyl Methacrylate
<b>HEA</b>	: 2-Hydroxy Ethyl Acrylate
<b>SPMAP</b>	: 3-Sulfo Propyl Methacrylate Potassium Salt
<b>SAPMA</b>	: 3-Sulfo Propyl Methacrylic Acid
<b>SAPMA-TEA</b>	: 3-Sulfo Propyl Methacrylic Acid Triethyl Amine
<b>VPA</b>	: Vinyl Phosphonic Acid
<b>GMA</b>	: Glycidyl Methacrylate
<b>EGMAP</b>	: Ethylene Glycidyl Methacrylate Phosphate
<b>AMPS</b>	: 2-Acrylamido-2-Methyl-Propansulfonic Acid
<b>SA</b>	: Styrene Sulfonic Acid
<b><i>t</i>BA-EDA</b>	: Tertiary Butyl Acrylate-Ethylene Diamine
<b>MMA</b>	: Methyl Methacrylate
<b>DMAEMA</b>	: 2-Dimethylaminoethyl Methacrylate
<b>TSA</b>	: p-Toluenesulfonic Acid Monohydrate
<b>CMS</b>	: p-Chloromethyl Styrene
<b>NIPAAM</b>	: N-Isopropylacrylamide
<b>EBB</b>	: 2-Bromoiso Butyrate
<b>EOMA</b>	: Oxyethylene Methacrylate
<b>BIEA</b>	: 2-(2-Bromoisobutyryloxy) Ethyl Acrylate
<b>NASS</b>	: Sodium 4-styrenesulfonate
<b>VBC</b>	: Vinyl Benzyl Chloride
<b>BTMA</b>	: Benzyl Trimethylammonium
<b>BTMAC</b>	: Benzyl Trimethylammonium Chloride
<b>PMDETA</b>	: N,N,N',N'',N'''-pentamethyldiethylenetriamine
<b>Me<sub>6</sub>-TREN</b>	: Tris[2-(dimethylamino) ethyl]amine
<b>DMF</b>	: Dimethyl Formamide
<b>NMP</b>	: N-Methyl-2-pyrrolidone
<b>TFA</b>	: Trifluoroacetic Acid
<b>Et<sub>3</sub>N</b>	: Triethylene Amine
<b>EDA</b>	: Ethylene Diamine
<b>ATR FT-IR</b>	: Total Reflection Fourier Transform Infrared Spectroscopy
<b>SEM</b>	: Scanning Electron Microscopy
<b>EDX</b>	: X-Ray Spectroscopy
<b>TGA</b>	: Thermogravimetric Analysis
<b>GPC</b>	: Gel Permeation Chromatography
<b>AFM</b>	: Atomic Force Microscopy

**DCS** : Differential Scanning Calorimetre  
**NMR** : Nuclear Magnetic Resonance  
**HMTETA** : Hexamethyltriethylene Tetraamine  
**TMEDA** : Tetramethylethylene Diamine

## LIST OF TABLES

	<u>Page No</u>
<b>Table 2.1</b> Monomers used in commercial fluoropolymers .....	4
<b>Table 2.2</b> The most frequently used initiator types in ATRP systems .....	23
<b>Table 3.1</b> Monomers used in PVDF-based graft copolymerization.....	36
<b>Table 3.2</b> Modified monomers used in PVDF-based graft copolymerization ...	37
<b>Table 3.3</b> As macroinitiator PVDF and its commercial structure, Nafion-117...	37
<b>Table 4.1</b> Reaction conditions and results of PVDF-based graft copolymers ...	50
<b>Table 4.2</b> Thermal decomposition temperatures of PVDF-based copolymers...	51

## LIST of FIGURES

	<u>Page No</u>
<b>Figure 2.1</b> : Various ways of obtaining fluorinated graft copolymers by grafting from technique.....	7
<b>Figure 2.2</b> : Schematic representation of the induced graft copolymerization of AA .....	9
<b>Figure 2.3</b> : Synthesis of branched copolymer PVDF- <i>g</i> -PBIEA- <i>g</i> -NaPSS .....	10
<b>Figure 2.4</b> : Synthesis of PVDF- <i>g</i> -PSSA graft copolymer.....	12
<b>Figure 2.5</b> : Synthesis of PVDF- <i>g</i> -PVBC graft copolymers.....	13
<b>Figure 2.6</b> : Synthesis of PVDF- <i>g</i> -(PVBC- <i>g</i> -PS) by ATRP.....	14
<b>Figure 2.7</b> : Formula of PVDF- <i>g</i> -PBTMAC graft copolymer.....	14
<b>Figure 2.8</b> : Synthesis of PVDF- <i>g</i> -PMMA and PVDF- <i>g</i> -POEM.....	16
<b>Figure 2.9</b> : Free radical chain process.....	18
<b>Figure 2.10</b> : Sequential-controlled radical polymerization.....	19
<b>Figure 2.11</b> : Transition metal catalyzed ATRP.....	21
<b>Figure 2.12</b> : Nitrogen based ligands.....	24
<b>Figure 2.13</b> : Derivatives of 2,2-Bipyridine.....	25
<b>Figure 2.14</b> : The rate equation of copper-based ATRP.....	26
<b>Figure 2.15</b> : Kinetic plot and conversion vs. time plot for ATRP.....	27
<b>Figure 2.16</b> : Scheme of AGET-ATRP .....	30
<b>Figure 2.17</b> : The Ford Focus FCV is Ford's most recent hydrogen car.....	31
<b>Figure 2.18</b> : Schematic representation of a typical PEMFC.....	32
<b>Figure 2.19</b> : Structure of Nafion-117.....	32
<b>Figure 4.1</b> : Synthesis of PVDF- <i>g</i> - <i>Pt</i> BA graft copolymer.....	51
<b>Figure 4.2</b> : Synthesis of PVDF- <i>g</i> -PAA graft copolymer.....	52
<b>Figure 4.3</b> : ATR FT-IR spectrum of PVDF- <i>g</i> -PAA graft copolymer.....	52
<b>Figure 4.4</b> : TGA and DSC Graphics of PVDF-107 and Nafion-117.....	53
<b>Figure 4.5</b> : TGA Graphics of PVDF-107 and PVDF- <i>g</i> -PAA Graft Copolymer ..	54
<b>Figure 4.6</b> : Synthesis of PVDF- <i>g</i> -PSPMAP Graft Copolymer .....	55
<b>Figure 4.7</b> : ATR FT-IR Spectrum of PVDF- <i>g</i> -PSPMAP graft copolymer.....	55
<b>Figure 4.8</b> : Synthesis of SAPMA monomer.....	56
<b>Figure 4.9</b> : Synthesis of SAPMA-TEA monomer .....	56
<b>Figure 4.10</b> :Synthesis of PVDF- <i>g</i> -PSAPMA-TEA graft copolymer.....	57
<b>Figure 4.11</b> : TGA and DSC graphics of PVDF-107 and PVDF- <i>g</i> -PSAPMA-TEA graft copolymer.....	57
<b>Figure 4.12</b> : Synthesis of PVDF- <i>g</i> -PHEMA graft copolymer.....	58
<b>Figure 4.13</b> : ATR FT-IR Spectrum of PVDF- <i>g</i> -PHEMA graft copolymer.....	59
<b>Figure 4.14</b> : TGA and DSC graphics of PVDF-107 and PVDF- <i>g</i> -PHEMA graft copolymer.....	60
<b>Figure 4.15</b> : <sup>1</sup> H NMR (d-DMF) spectrum of PVDF- <i>g</i> -PHEMA graft copolymer	60
<b>Figure 4.16</b> : Synthesis of PVDF- <i>g</i> -PS graft copolymer .....	61
<b>Figure 4.17</b> : GPC graphic of PVDF-107.....	62

<b>Figure 4.18</b> GPC chromatograms of PVDF-107 (RI detector) and PVDF- <i>g</i> -PS (RI detector) graft copolymer.....	62
<b>Figure 4.19</b> : ATR FT-IR spectrum of macroinitiator PVDF-107 and PVDF- <i>g</i> -PS graft copolymer.....	63
<b>Figure 4.20</b> : <sup>1</sup> H NMR (d-DMF) spectrum of PVDF- <i>g</i> -PS graft copolymer.....	64
<b>Figure 4.21</b> : Synthesis of PVDF- <i>g</i> -PSA graft copolymer.....	64
<b>Figure 4.22</b> : <sup>1</sup> H NMR (d-DMF) spectrum of PVDF- <i>g</i> -PSA graft copolymer.....	65

## PVDF-BASED GRAFT COPOLYMERS

### SUMMARY

During the last two decades, many special fluoropolymers have been developed, due to their chemical resistance, low surface free energy properties and oil/water repellence due to their hydrophobic properties. Amphiphilic fluorinated graft copolymers are of considerable interest for proton exchange membrane applications.

The limitations to the most known commercial membranes are a susceptibility to chemical degradation at elevated temperature, including poor ionic conductivities at low humidity or elevated temperatures, finally, membrane expensiveness. Thus synthesizing alternative membranes for fuel cells is still a challenging goal.

Poly (vinylidene fluoride) (PVDF) has commercial importance due to its excellent resistance to chemicals, weathering elements and oxidants, as well as for special properties such as resistance. Because of its commercial importance, various synthetic approaches for the preparation of graft copolymers from PVDF have been reported.

Atom transfer radical polymerization (ATRP) and activators generated by electron transfer (AGET)-ATRP are controlled free radical polymerization techniques. These techniques also permit advanced fluorinated materials to be synthesized. They are one of the best route for the preparation of these well-defined amphiphilic graft copolymers with controlled molecular weight, polydispersity, terminal functionalities, and chain architecture composition due to the relative ease of synthesis and their compatibility with a wide range of solvents.

In this study, graft copolymers of PVDF were synthesized by ATRP and AGET-ATRP. Additionally, ionic functionality containing monomers was also synthesized by hydrolysis reaction.

In the graft copolymerization *tert*-butyl acrylate (*t*BA), 3-sulfo propyl methacrylate, potassium salt (SPMAP), 2-hydroxy ethyl methacrylate (HEMA), 2-hydroxy-ethyl acrylate (HEA), vinyl phosphoric acid (VPA), 2-acrylamido-2-methyl-1-propane sulphonic acid (AMPS), ethylene glycdyl methacrylate phosphate (EGMAP), glycdyl methacrylate (GMA), styrene (S) and synthesized monomers such as 3-sulfo propyl methacrylic acid three ethyleneamine (SAPMA-TEA), was used as monomers using PVDF as a macro-initiator in the presence of different catalyst complex and reaction conditions.

The PVDF-based graft copolymers were characterized using gel permeation chromatography (GPC) for determining the molecular weight shift, <sup>1</sup>H NMR (d-DMF) for compositions, Total Reflection Fourier Transform Infrared Spectroscopy (ATR FT-IR) spectroscopy for structure, differential scanning calorimetry (DSC), thermo gravimetric analysis (TGA) for thermal properties.

## PVDF KÖKENLİ AŞI KOPOLİMERLER

### ÖZET

Son on yıl içersinde flor içeren birçok özel kopolimerlerin sentezlenmesinin sebebi, flor içeren kopolimerlerin çok düşük serbest yüzey enerjilerine sahip olmaları ve hidrofob özelliklerinden dolayı su/yağı üzerlerinde tutmamalarıdır. Amfifilik flor içeren aşı kopolimerlerin de pek çok uygulama alanları vardır. Proton değişim yakıt pillerinin membran sentezinde flor içeren kopolimerler önemli bir yer tutmaktadır.

En yaygın ticari yakıt pillerinin membranlarının yüksek sıcaklıklarda kimyasal bozunmaya eğilimli olmaları, yüksek sıcaklık ve düşük nemde düşük proton iletkenliğine sahip olmaları ve pahalı olmaları mevcut ticari membranlara alternatif membranların araştırılmasına neden olmaktadır.

Poli(viniliden florür) (PVDF) 'ün kimyasallara, oksidantlara ve aşınmaya karşı yüksek direnç gösteriyor olması ticari olarak son derece yaygın bir malzeme olarak kullanılmasına neden olmaktadır. PVDF'in ticari öneminden dolayı PVDF kökenli aşı kopolimerleri için farklı sentez yöntemleri denenmiştir.

Atom transfer radikal polimerizasyon (ATRP) ve aktivatörlerin elektron transferi yolu ile oluşturulduğu (AGET)-ATRP, kontrollü serbest radikal polimerizasyon yöntemleridir. Bu yöntemler iyi tanımlanmış, molekül ağırlığı kontrol edilebilen, düşük molekül ağırlığı dağılımına sahip, uç grup fonksiyonlitesi içeren ve farklı kompozisyonlarda zincir yapısından oluşan polimerleri ve özellikle ampifilik aşı kopolimerleri kolay sentez edebilmek için kullanılan ve bilinen çoğu çözücüler ile uyumlu en iyi yoldur.

Bu çalışmada, PVDF kökenli aşı kopolimerleri ATRP ve AGET-ATRP yöntemleri kullanılarak sentezlenmiştir. Ayrıca hidroliz reaksiyonu kullanılarak iyonik fonksiyonel grup içeren monomerler de sentezlenmiştir.

ATRP ve AGET-ATRP koşullarında tersiyer bütül akrilat (*t*BA), 3-sulfo propil metakrilat, potasyum tuzu (SPMAP), 2-hidroksi etil metakrilat (HEMA), 2-hidroksi etil akrilat (HEA), vinil fosforik asit (VPA), 2-akrilomido-2-metil-1-propan sulfonik asit (AMPS), etilen glisidil metakrilat fosfat (EGMAP), glisidil metakrilat (GMA), stiren (S) ve sentezlenmiş olan 3-sulfo propil metakrilik asit trietilenamin (SAPMA-TEA) monomer olarak kullanılarak aşı kopolimerizasyonu gerçekleştirilmiştir.

Sentezlenen aşı kopolimerleri molekül ağırlığı için jel geçirgenlik kromatografisi (GPC), yapı için nükleer manyetik rezonansı (<sup>1</sup>H-NMR) (d-DMF) ve Fourier transfer infrared spektrometresi (ATR FT-IR) ve termal özellikleri differansiyel tarama kalorimetrisi (DSC), termal ağırlık analizi (TGA) ölçümleri kullanılarak karakterize edilmiştir.

## 1. INTRODUCTION

Fluorinated polymers have always attracted significant attention due to their high thermal stability, good chemical resistance, and excellent mechanical properties at extreme temperatures, superior weatherability, oil and water repellence and low flammability in addition to low refractive index. Several attempts have been reported to prepare semi-fluorinated copolymers by means of cationic, anionic, living radical, and group transfer polymerisation, but these techniques have been limited by the need for high-purity monomers and solvents, reactive initiators and anhydrous conditions. [1] The development of fluoropolymers began with the invention of polytetrafluoroethylene (PTFE) in 1938 by Dr. Roy Plunkett of DuPont Company, continuing in 1992 when a soluble perfluoropolymer (Teflon AF) was invented. Besides these commercially important examples both academic and industrial teams have researched many other routes toward fluorinated materials intensively. These efforts have led to the emergence of various functional materials with notable properties such as proton conducting membranes for fuel cell. The most investigated proton exchange membranes (PEM) are based on fluorinated polymers and, in particular, the DuPont Nafion117.

The fluorinated backbone of fluorinated polymers possesses the chemical, mechanical and thermal resistivity to the molecule, the ionizable end groups at the side chain has high proton permeability and cation transfer capacity properties. The limitations to large-scale commercial use include poor ionic conductivities at low humidities and/or elevated temperatures, a susceptibility to chemical degradation at elevated temperatures and finally, cost.

In order to overcome the limitations, many other alternative polymers have been tested during these years. The partially fluorinated polymer poly (vinylidene fluoride) (PVDF) based proton exchange membranes seem to offer the most promising performances. Because of PVDFs advantages many methods for preparing PVDF based graft copolymers received attention.

PVDF has a commercial importance due to its excellent resistance to chemicals, weathering elements and oxidants. Because of its commercial importance, various synthetic approaches for the preparation of graft copolymers from partially fluorinated poly (vinylidene fluoride) (PVDF) have been reported [6].

Methods for preparing PVDF based graft copolymers are generally classified: (1) the grafting through; (2) the grafting from; (3) the grafting onto methods. The most used method is “grafting from” method. Grafting from method has main techniques: (i) by the irradiation ii) by transfer to the polymer; (iii) by ozonization of PVDF (iv) by the direct terpolymerization of two fluoroalkenes. [4] To avoid the drawbacks of the grafting from method techniques, the controlled radical polymerization methods was used and has become one of the most useful techniques for the synthesis of graft polymers. [5] Atom transfer radical polymerization (ATRP) and activator generated by electron transfer (AGET)-ATRP are one of the controlled free radical polymerization techniques.

ATRP is one of the most versatile methods for synthesizing homopolymers and copolymers with predetermined molecular weights and narrow molecular weight distributions. It is based on the combination of an organic halide initiator (RX) with a metal/ligand catalytic system, which is able to promote fast initiation compared to propagation and then reversibly activate halogenated chain, ends ( $P_nX$ ) during polymerization. AGET-ATRP has a significant advantage according to ATRP, because it provides a route for synthesizing pure functional polymeric materials of any desired architecture and AGET-ATRP initiation is that the reducing agent used to remove dissolved oxygen from the system and hence the reaction can be conducted in a limited amount of air. [32]

In this study PVDF based graft copolymers were synthesized by using ATRP and AGET-ATRP, also functional group containing ionic monomers was synthesized by hydrolysis reaction.

In the graft copolymerization *tert*-butyl acrylate (*t*BA), 3-sulfo propyl methacrylate, potassium salt (SPMAP), 2-hydroxy ethyl methacrylate (HEMA), 2-hydroxy-ethyl acrylate (HEA), vinyl phosphoric acid (VPA), 2-acrylamido-2-methyl-1-propane sulphonic acid (AMPS), ethylene glycidyl methacrylate phosphate (EGMAP),

glycidyl methacrylate (GMA), styrene (S) and synthesized monomers such as 3-sulpho propyl methacrylic acid three ethyleneamine (SAPMA-TEA), was used as monomers using PVDF as a macro-initiator in the presence of different catalyst complex and reaction conditions.

The PVDF-based graft copolymers were characterized using gel permeation chromatography (GPC) for determining the molecular weight shift, <sup>1</sup>H NMR (d-DMF) for compositions, Total Reflection Fourier Transform Infrared Spectroscopy (ATR FT-IR) spectroscopy for structure, differential scanning calorimetry (DSC), thermo gravimetric analysis (TGA) for thermal properties.

## 2. THEORETICAL PART

### 2.1 Fluoropolymers

Fluoropolymers represent a rather specialized group of polymeric materials. The development of fluoropolymers began with the invention of polytetrafluoroethylene (PTFE) in 1938 by Du Pont Company, continuing in 1992 when a soluble perfluoropolymer (Teflon<sup>®</sup> AF) was invented. Besides these commercially important examples, a large number of new types of fluoropolymers have been developed and a relatively high proportion of those in the last two decades.

Monomers for commercially important large-volume fluoropolymers and their basic properties are shown in Table 2.1. These can be combined to yield homopolymers, copolymers, and terpolymers.

**Table 2.1** Monomers Used in Commercial Fluoropolymers

Ethylene	$\text{CH}_2=\text{CH}_2$
Tetrafluoroethylene	$\text{CF}_2=\text{CF}_2$
Chlorotrifluoroethylene	$\text{CF}_2=\text{CClF}$
Vinylidene fluoride	$\text{CH}_2=\text{CF}_2$
Vinyl fluoride	$\text{CFH}=\text{CH}_2$
Propene	$\text{CH}_3\text{CH}=\text{CH}_2$
Hexafluoropropene	$\text{CF}_3\text{CF}=\text{CF}_2$
Perfluoromethylvinyl ether	$\text{CF}_3\text{OCF}=\text{CF}_2$
Perfluoropropylvinyl ether	$\text{CF}_3\text{CF}_2\text{CF}_2\text{OCF}=\text{CF}_2$

The three principal strategies developed for the synthesis of functional fluoropolymers. The first concerns the direct radical copolymerization of fluoroalkenes with fluorinated functional monomers. The latter are either fluorinated

vinyl ethers, a,b,b-trifluorostyrenes or trifluorovinyl oxy aromatic monomers bearing sulfonic or phosphonic acids. The second route deals with the chemical modification of hydrogenated polymers (e.g. polyparaphenylenes) with fluorinated sulphonic acid synthons. The third alternative concerns the synthesis of FP-g-poly(M) graft copolymers where FP and M stand for fluoropolymers and monomer, respectively, obtained by activation (e.g. irradiation arising from electrons, g-rays, or ozone) of FP polymers followed by grafting of M monomers. The most used M monomer is styrene, and a further step of sulfonation on FP-g-PS leads to FP-g-PS sulfonic acid graft copolymers. Synthesized fluoropolymers are generally characterized by using transmission electron microscopy (TEM), atomic-force microscopy (AFM), light scattering, fluorescence spectroscopy, small-angle neutron scattering (SANS), small-angle X-ray scattering (SAXS), potentiometric titration, microcalorimetry, TGA, DSC and electrokinetic analyzer.

Fluoropolymers are widely used in chemical, automotive, electrical, and electronic industries; in aircraft and aerospace; in communications, construction, medical devices, special packaging, protective garments, and a variety of other industrial and consumer products. They represent a group of macromolecules offering a variety of unique properties, in particular, a good-to-outstanding chemical resistance and stability at elevated temperatures.

In contrast to hydrogenated polymers, fluoropolymers are potential candidates due to their outstanding properties that open various applications. The small size and the high electronegativity of the fluorine atom confers a strong C–F bond and a low polarizability. Such polymers show low intermolecular interactions, which leads to low cohesive energy, and therefore, to low surface energy. They also exhibit high thermostability and chemical inertness, low refractive index and friction coefficient, good hydrophobicity and lipophobicity, valuable electrical properties, and low relative permittivity. In addition, they are non-sticky and resistant to UV, to ageing and to concentrated mineral acids and alkalies. [1] On the other hand, they exhibit some deficiencies when compared with most engineering polymers. They typically have poorer mechanical properties, higher permeability, and often considerably higher cost.

In order to overcome the deficiencies of fluoro polymers, many other alternative polymers have been tested during these years. Today, the poly (vinylidene fluoride)

(PVDF) and PVDF-based graft copolymers seem to offer the most promising performances, combining high room temperature proton conductivity, chemical stability, low permeability, and resistance to nuclear radiations, and good mechanical properties.

## 2.2 PVDF-Based Graft Copolymers

Poly(vinylidene fluoride) (PVDF) has been known since the 1960`s for its excellent mechanical and physicochemical properties. It has found widespread industrial applications and research interests [2]. PVDF comprises alternating  $-CH_2$  and  $-CF_2$  groups. These alternating units can crystallize with larger  $-CF_2$  groups adjacent to smaller  $-CH_2$  units on an adjacent chain. This interpenetration gives rise to high modulus. In fact, PVDF has the highest flexural modulus of all fluoropolymers. The above alternating groups create a dipole that renders the polymer soluble in highly polar solvents, such as dimethyl formamide (DMF), dimethyl sulphoxide (DMSO), trifluorotoluene and dimethylacetamide. Other consequences of this structure are a high dielectric constant and high dielectric loss factor and piezoelectric behavior under certain conditions. The shielding effect of the fluorine atoms adjacent to the  $-CH_2$  groups provides the polymer with a good chemical resistance and thermal stability. [3]

In addition, PVDF is not toxic and less expensive than other fluoropolymers such as poly(chlorotrifluoroethylene), poly(trifluoroethylene) or poly(tetrafluoroethylene). Thus, graft copolymers containing a PVDF backbone would be particularly interesting, and potentially useful, because the incorporation of PVDF would raise the chemical resistance and thermal stability of the polymer and should lower the surface energy. On the other hand, PVDF is hydrophobic in nature; therefore, in order to confer hydrophilic properties and, consequently, proton conductivity, a chemical modification by means of grafting is needed.

Graft copolymers have received much attention as “novel polymeric materials” with multi-components, since they are made of different polymeric sequences linked together. It is well known that heterogeneous graft copolymers tend to show the properties of both (or more) polymeric backbone and the oligomeric or polymeric grafts rather than averaging the properties of both homopolymers.

Basically, three different methods enable one to synthesize fluorinated graft copolymers, recently summarized: (1) the grafting through; (2) the grafting from; (3) the grafting onto routes. There are different ways to obtain graft copolymers by grafting from” method: (i) by the irradiation (plasma, swift heavy ions, X-rays, or electron beam, mainly under  $\gamma$  rays or  $^{60}\text{Co}$  source) of fluoropolymers followed by a grafting (that strategy was extensively used by Holmberg et al. who synthesized PVDF-*g*-poly(styrene sulphonic acid) graft copolymers for fuel cell membranes); (ii) by transfer to the polymer; (iii) by ozonization of PVDF . By ozone activation of PVDF, Boutevin’s team prepared PVDF-*g*-poly(M) where M represents styrene, acrylic acid, dimethylaminoethyl methacrylate, or phosphonated monomers. [4] (iv) by the direct terpolymerization of two fluoroalkenes such as VDF and chlorotrifluoroethylene (CTFE) with *tert*-butylallyl peroxycarbonate at low temperature leading to terpolymers bearing peroxycarbonate dangling groups. Hence, these original macroinitiators were able to initiate the radical polymerization of VDF to yield poly(VDF-*co*-CTFE)-*g*-PVDF graft copolymers as original thermoplastic elastomers. However, not all these above methods allow assessing the molecular weights of the graft segments.

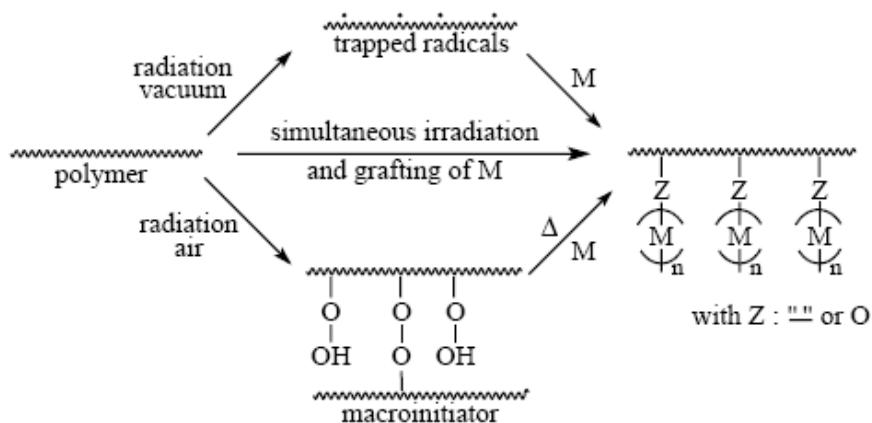


**Figure 2.1.** Various Ways of Obtaining Fluorinated Graft Copolymers by Grafting From Technique.

To avoid this drawback, the controlled radical polymerization was used and has become one of the most useful strategies for the synthesis of graft polymers while this technique was also successful in achieving fluorinated block copolymers from initiators containing C-I, C-Br, and C-Cl bonds. It was reported the synthesis of graft copolymer by reversible addition-fragmentation chain transfer polymerization (RAFT) to obtain original PVDF-*g*-PMMA and PVDF-*g*-poly (acrylic acid) (PVDF-

*g*-PAA) graft copolymers. It was prepared PVDF-*g*-PAA and PVDF-*g*-PAA-*b*-PNIPAAm copolymers by RAFT polymerization of AA with an ozone-pretreated PVDF. [5]

A significant disadvantage of these free radical techniques is that homopolymerization of the comonomer always occurs to some extent, resulting in a product which is a mixture of graft copolymer and homopolymer. Moreover, backbone degradation and gel formation can occur as a result of uncontrolled free radical production, often limiting the attainable grafting density [6].

Indeed, ATRP is regarded as one of the most efficient controlled polymerization methods to prepare polymers and copolymers endowed with different architectures and low polydispersities. [5]

### **2.2.1 Synthesis of PVDF-Based Graft Copolymers by Ozone Activated PVDF**

Ozone, commonly written O<sub>3</sub>, is an inexpensive gas (quite soluble in fluorinated solvents), but it is well known for environmental concerns. The ozonization allows the activation of a wide range of polymers, mainly polyolefin (polyethylene, polypropylene, PVC) but also PS, poly (dienes), PDMS, polyurethanes, PVDF and finally copolymers.

The direct oxidation of polymer chains by ozone is a well-known method for introducing peroxides and hydroperoxides for the subsequent graft polymerization. Generally, the amount of peroxides introduced into a polymer sample by ozone treatment can be regulated by the treatment temperature, ozone concentration, and treatment time. [7] PVDF graft copolymers were synthesized in a two step-procedure: first step is the ozone treatment of PVDF, final step is monomer grafting or grafting the ozone activated PVDF to a polymer.

#### **2.2.1.1 Synthesis of PVDF-*g*-PAA Graft Copolymer by Radical-Induced Polymerization**

Molecular modification of ozone-pretreated PVDF via thermally induced graft copolymerization with acrylic acid (AA) in *N*-methyl-2-pyrrolidone (NMP) solution was carried out (the PVDF -*g*-PAA copolymer). The microstructure and composition of the PVDF -*g*-PAA copolymers were characterized by FT-IR, X-ray photoelectron spectroscopy (XPS), elemental analysis, and thermo gravimetric (TG) analysis. In general, the graft concentration increased with the AA monomer concentration used

for graft copolymerization. PVDF powders in solution activated by fixed  $O_3/O_2$  mixture concentration at room temperature 15 min. This pretreatment time gives rise to a peroxide content of about  $10^{-4}$  mol/g of the polymer. The peroxides on the activated PVDF chains are used as initiators for the subsequent radical-induced graft polymerization of AA. The initiator decomposition is the rate-limiting step in radical polymerization. Based on these data, the half-life for the decomposition of peroxides on the ozone-treated PVDF was estimated to be about 45 min at 60 °C. Thus, a polymerization time of 3 h at 60 °C should be sufficient for the complete decomposition of the peroxides.

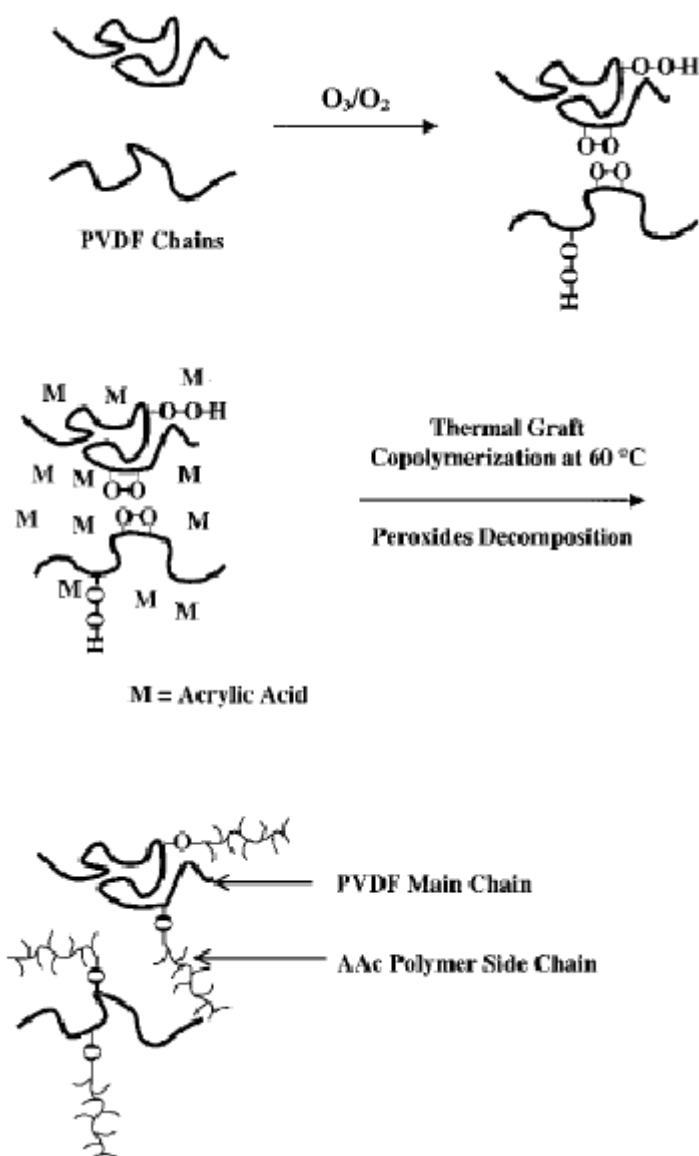


**Figure 2.2.** Schematic Representation of The Induced Graft Copolymerization of AA

### 2.2.1.2 Synthesis of PVDF-g-PPEOMA Graft Copolymer by ATRP

Amphiphilic graft copolymers prepared using ozone penetrated PVDF incorporating poly(oxyethylene methacrylate)( PEOMA), a hydrophilic macromonomer. Under the grafting conditions a limiting grafting density of 23-wt % comonomer was obtained [6]. The polymerization carried out at 100 °C in NMP from [PEOMA]: [PVDF] with weight ratio ranging from 1:1 to 6:1. The structures of the resulting PVDF-g-PPEOMA graft copolymers were investigated by FTIR and XPS, showing, as expected, that the graft concentration increased with increasing PEOMA macromonomer concentration. [1]

### 2.2.1.3 Synthesis of PVDF-g-PBIEA-g-NaPSS, PVDF-g-PBIEA-g-PEGMA, PVDF-g-PBIEA-g-PDMAEMA Graft Copolymers by ATRP

2-(2-Bromoisobutyryloxy) ethyl acrylate (BIEA) was polymerized on the surface of ozone-pretreated PVDF and further used as macroinitiator for functional monomers sodium 4-styrenesulfonate sodium 4-styrenesulfonate (NaSS) and PEGMA ( $M_n \sim 360$  g/mol) to yield branched graft copolymers (Fig. 2.3). Copolymers of PVDF-g-PBIEA-g-NaPSS cast in 1 M aq. NaCl solution were enriched in sodium 4-styrenesulfonate (NaPSS) side chains on the surface. PVDF-g-PBIEA copolymers were used to run ATRP of EGMA and the resulting PVDF-g-PBIEA-g-PEGMA copolymers. 2-dimethylaminoethyl methacrylate (DMAEMA) was also polymerized by ATRP from a PVDF-g-PBIEA copolymer and the resulting PVDF-g-PBIEA-g-PDMAEMA copolymer. [1]

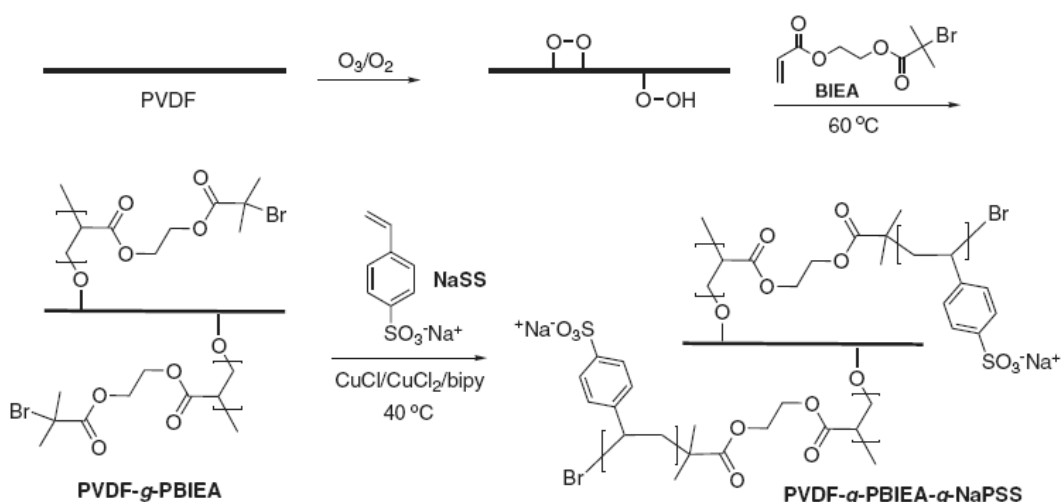


**Figure 2.3.** Synthesis of Branched Copolymer PVDF-g-PBIEA-g-NaPSS

#### **2.2.1.4 Synthesis of PVDF-g-PAA-b-PNIPAAm and PVDF-g-PEGMA Copolymers by RAFT**

PVDF with “living” PEGMA ( $M_n \sim 300$  g/mol) side chains (PVDF-g-PEGMA) were prepared through molecular graft copolymerization of the PEGMA macromonomer with ozone-preactivated PVDF backbone in a RAFT-mediated process.

PVDF-g-PAA copolymers with well-defined PAA side chains were synthesized by RAFT-mediated graft copolymerization of acrylic acid with ozone-pretreated PVDF. The PVDF-g-PAA copolymers were further functionalized in a subsequent surface-initiated block copolymerization with N-isopropylacrylamide (NIPAAm) resulting PVDF-g-PAA-*b*-PNIPAAm copolymer. [1]

#### **2.2.2 Synthesis of Graft Copolymers by Irradiated PVDF**

Radiation induced grafting can also be used for the synthesis of original graft copolymers. For this method, a polymer endowed with the required mechanical, chemical or thermal properties is irradiated with electron beams or  $\gamma$ -rays (usually emitted from various radioactive isotopes:  $^{60}\text{Co}$  obtained by beaming  $^{59}\text{Co}$  with neutrons in a nuclear reactor, and  $^{137}\text{Cs}$  which is a product of fission of  $^{235}\text{U}$ ). Generally, the use of an electron beam enables activation on the surface. Hence, the polymer to be activated can first be processed into thin films. By contrast, irradiation is efficient in the bulk of the substrate and thicker films can hence be treated. The irradiation causes free radical centers formed in the polymeric matrix.

Different types of high-energy radiation are available for use in the grafting process, although crosslinking may occur, the radiation-chemical effects in PVDF showed that crosslinking proceeds mainly through an alkyl macroradical. This radiation may be either electromagnetic, such as X-rays and  $\gamma$ -rays, or charged particles, such as  $\beta$  particles or electrons.

Radical generation throughout the film thickness is necessary. Fortunately, all of the radiation discussed above has sufficient energy to penetrate into the bulk of fluorinated films, which are usually 25–200  $\mu\text{m}$  thick.

The irradiation and grafting can be carried out in one step, in two, or in more steps.

This remainder of this sub-section is divided into two parts: (i) investigations on the activation of fluorinated homopolymers followed by the grafting, and (ii) methods starting from the irradiation of fluorinated copolymers, with a subsequent grafting.



C–H and C–F branch sites of PVDF. Grafting was assumed to take place in the amorphous regions of PVDF. The sulfonation step was realized in high yields (up to 100 %), occurring mainly in the para position of the phenyl ring. These novel films were characterized by Raman and NMR spectroscopy, wide angle X-ray scattering (WAXS), and small angle X-ray scattering (SAXS). [1]

### 2.2.2.2 Synthesis of PVDF-*g*-PVBC Graft Copolymer

PVDF-*g*-PVBC copolymers was synthesized in a two step-procedure: first, PVDF was activated under nitrogen atmosphere by  $\gamma$  ray from a  $^{60}\text{Co}$  source at a dose of 6.3 Mrad, at 70 °C for 1 week, the final step is the grafting of VBC monomer. [1]

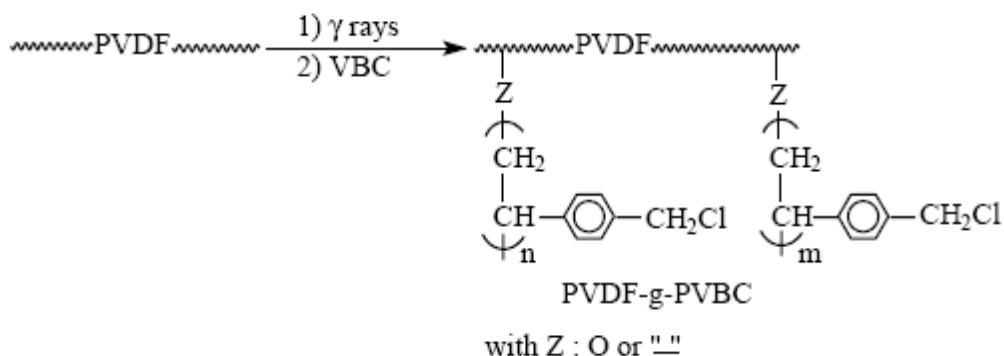


**Figure 2.5.** Synthesis of PVDF-*g*-PVBC Graft Copolymers

PVDF-*g*-PVBC copolymers (Figure 2.5), where VBC stands for vinyl benzyl chloride, acted as suitable macroinitiators via their chloromethyl side groups in ATRP of styrene, with a copper bromide/bipyridine catalytic system, leading to control PVDF-*g*- [PVBC-*g*-PS] graft copolymers, as in figure 2.6. The high degree of grafting achieved would not be possible with conventional uncontrolled radiation induced grafting methods owing to termination reactions. The polystyrene grafts were sulfonated, leading to well-defined PVDF-*g*- [PVBC-*g*-PSSA] copolymers.

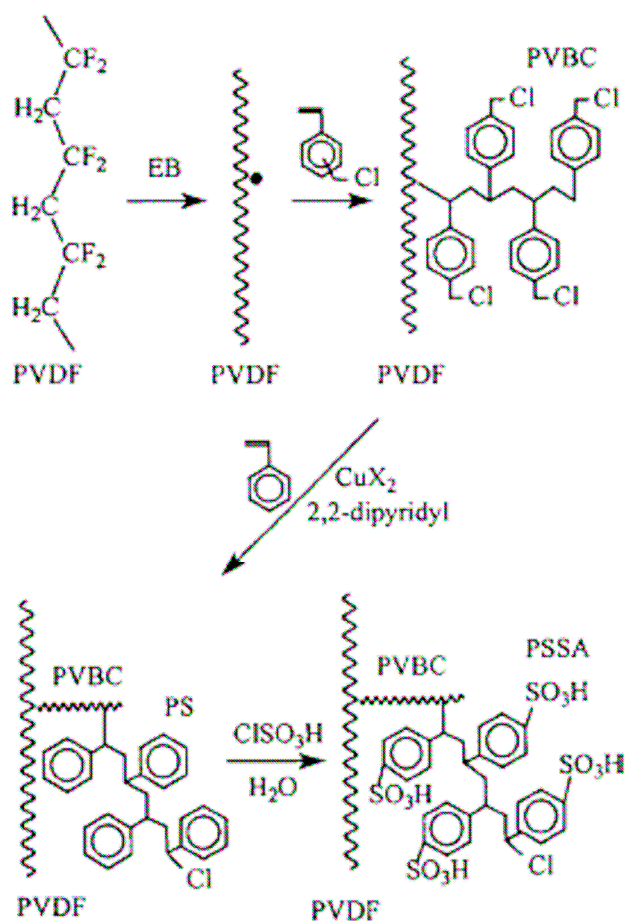


**Figure 2.6.** Synthesis of PVDF-g-(PVBC-g-PSSA) by ATRP

The chloromethyl end groups of PVDF-g-PVBC copolymers underwent an amination reaction into benzyl trimethylammonium (BTMA) hydroxide or BTMA chloride (BTMAC) for PVDF-g-PBTMAC graft copolymers. (Figure 2.7)

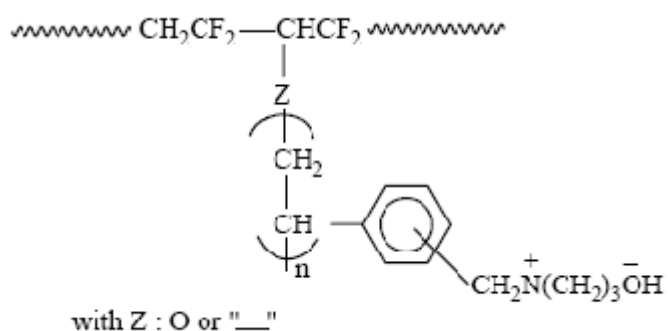


**Figure 2.7.** Formula of PVDF-g-PBTMAC Graft Copolymer

### **2.2.2.3 Synthesis of PVDF-g-PMMA Graft Copolymer**

Poly(methyl methacrylate) (PMMA) was anchored to PVDF film surface via electron beam pre-irradiation grafting technique to prepare PVDF/PMMA brushes. The conformation of the PVDF/PMMA brushes was verified through attenuated total reflection-Fourier transform infrared spectroscopy (ATR-FTIR), energy dispersive X-ray spectroscopy (EDX), and scanning electron microscopy (SEM). Thermal stability of PVDF/PMMA brushes was characterized by thermo gravimetric analysis (TGA). [8]

### **2.2.2.4 Synthesis of PVDF-g-PCMS Graft Copolymer by ATRP**

PVDF-g-PCMS copolymers have been prepared by preirradiation grafting of p-chloromethylstyrene (CMS) solutions in toluene onto 80  $\mu\text{m}$  PVDF films. These copolymers were employed for ATRP of styrene with CuCl or CuBr and bipy at 120  $^{\circ}\text{C}$ . The polymerization increased linearly with time up to at least 400% PS grafting. This implicated first-order kinetics and a controlled radical polymerization. Finally, the PS grafts are sulfonated. SEM/EDX-ray results implied that the copolymers had to be grafted throughout the matrix with both PCMS and PS to become proton conducting after sulfonation. [1]

### **2.2.3. Synthesis of PVDF-Based Graft Copolymers by Direct Initiation of PVDF**

The direct initiation method using PVDF macroinitiator allows synthesizing graft copolymers with minimized homopolymer formation. [9] Direct initiation of the secondary fluorinated site of high molecular weight PVDF has been exploited in the preparation of amphiphilic graft copolymers. [1]

#### **2.2.3.1 Synthesis of PVDF-g-POEM, PVDF-g-PMMA Graft Copolymers by ATRP**

Amphiphilic copolymer derivatives of PVDF poly (oxyethylene methacrylate) (PVDF-g-POEM) side chains and having poly (methyl methacrylate) side chains (PVDF-g-PMMA) are prepared using this “grafting from” method. (Figure 2.8)

PVDF-g-POEM and PVDF-g-PMAA with high grafting density was prepared under moderate conditions, i.e., 30 $^{\circ}\text{C}$  and 30 min polymerization time, using 4,4-dimethyl-

2, 20-dipyridyl (DMDP) and tris(2-aminoethyl) amine (Me-TREN) as ligands; 1-methyl-2-pyrrolidinone (NMP) as solvent and CuCl as a coinitiator.

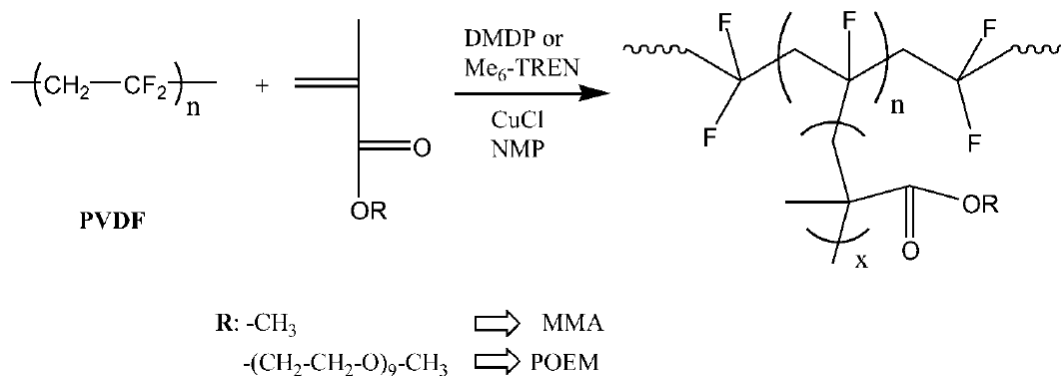


**Figure 2.8.** Synthesis of PVDF-*g*-PMMA and PVDF-*g*-POEM

Copolymers were characterized by gel-permeation chromatography (GPC), <sup>1</sup>H-NMR, DSC and AFM. Linear ln([M]<sub>0</sub>/[M]) vs. time and molecular weight vs. conversion plots confirm the living nature of the graft copolymerization. AFM on PVDF-*g*-POEM revealed a microphase-separated morphology characteristic of graft copolymers. [9]

### 2.2.3.2 Synthesis of PVDF-*g*-PMAA Graft Copolymer by ATRP

The preparation of PVDF-*g*-PMAA was a two-step synthesis. In the first step, poly(*tert*-butyl methacrylate) (*Pt*BMA) side chains were graft copolymerized onto PVDF using ATRP. In the second step, the *Pt*BMA side chains were hydrolyzed to yield polymethylmethacrylate (PMAA). It is well known that *Pt*BMA can be selectively and quantitatively hydrolyzed to PMAA in the presence of *p*-toluenesulfonic acid monohydrate (TSA). The combined GPC, TEM, NMR, and elemental analysis results indicate unambiguously that *Pt*BMA are grafted to the PVDF base polymer, hydrolyzed to PMAA, apparently by ATRP initiation at the secondary fluorinated site. [6]

### 2.2.4 Synthesis of PVDF-Based Graft Copolymers by Functionalised PVDF

Films of PVDF were treated by Liu et al. with LiOH to generate oxygen-containing functionalities on the polymer chains by elimination of HF followed by reduction, ultimately forming a PVDF functionalised with OH-groups on the surface. This was in turn reacted with ethyl 2-bromoisobutyrate (EBB) yielding a macroinitiator for

ATRP equipped for fashioning polymer brushes on the film surface. Brushes of MMA and PEGMA ( $M_n \sim 300$  g/mol) were synthesized successfully using CuBr/HMTETA and CuCl/CuCl<sub>2</sub>/bipy, respectively.

2-dimethylaminoethyl methacrylate (DMAEMA) was further copolymerized onto the PMMA and PEGMA brushes (CuBr/HMTETA) forming block copolymer grafts on the PVDF surface. [1]

### 2.3 Free Radical Polymerizations

Free radical polymerization (FRP) has many advantages over other polymerization processes. Free radical polymerizations are of significant importance in the industrial sector for a variety of reasons. First, many monomers capable of undergoing chain reactions are available in large quantities from the petrochemical sector [10]. In addition, free radical mechanisms are well understood and extension of the concepts to new monomers is generally straightforward. A third advantage of free radical routes is that the polymerization proceeds in a relatively facile manner: rigorous removal of moisture is generally unnecessary while polymerization can be carried out in either the bulk phase or in solution. However, the major limitation of FRP is poor control over some of the key elements of the process that would allow the preparation of well-defined polymers with controlled molecular weight, polydispersity, composition, chain architecture, and site-specific functionality.

As chain reactions, free radical polymerizations proceed via four distinct processes:

1. *Initiation*. In this first step, a reactive site is formed, thereby “initiating” the polymerization.
2. *Propagation*. Once an initiator activates the polymerization, monomer molecules are added one by one to the active chain end in the propagation step. The reactive site is regenerated after each addition of monomer.
3. *Transfer*. Occurs when an active site is transferred to an independent molecule such as monomer, initiator, polymer, or solvent. This process results in both a terminated molecule (see step four) and a new active site that is capable of undergoing propagation.
4. *Termination*. In this final step, eradication of active sites leads to “terminated,” or inert, macromolecules. Termination occurs via coupling reactions of two active

centers (referred to as combination), or atomic transfer between active chains (termed disproportionation).

The free radical chain process is demonstrated schematically below (Figure 2.9):  $R'$  represents a free radical capable of initiating propagation;  $M$  denotes a molecule of monomer;  $R_m$  and  $R_n$  refer to propagating radical chains with degrees of polymerization of  $m$  and  $n$ , respectively;  $AB$  is a chain transfer agent; and  $P_n + P_m$  represent terminated macromolecules.

Because chain transfer may occur for every radical at any and all degrees of polymerization, the influence of chain transfer on the average degree of polymerization and on polydispersity carries enormous consequences. Furthermore, propagation is a first order reaction while termination is second order. Thus, the proportion of termination to propagation increases substantially with increasing free radical concentrations. Chain transfer and termination are impossible to control in classical free radical processes, a major downfall when control over polymerization is desired.

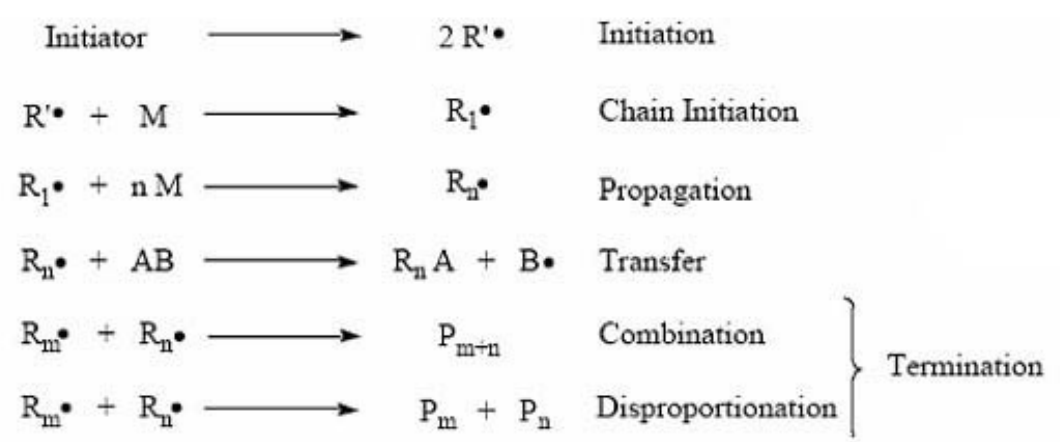


**Figure 2.9.** Free Radical Chain Process

### 2.3.1 Controlled / Living Radical Polymerizations

Generally, block copolymers can be prepared in a sequential fashion by the polymerization of one monomer, followed by a second monomer. This is also true for controlled radical polymerizations (Figure 2.10), which permit the synthesis of wide variety of block copolymers and maybe be more versatile than other living polymerization methods

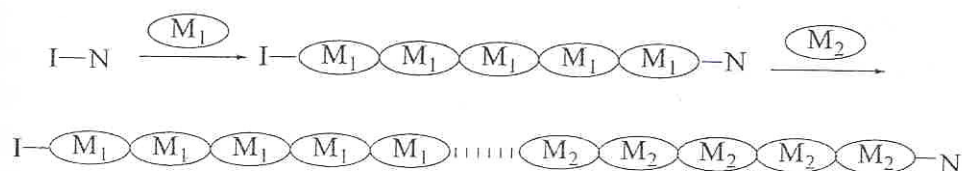


**Figure 2.10:** Sequential-Controlled Radical Polymerization

Sequential-controlled radical polymerization includes (1) the addition of the second monomer into the polymerization system of the first monomer without any isolation, and (2) the initiation of the polymerization of second monomer using a macroinitiator obtained from controlled radical polymerization of the first monomer.

The term controlled/“living” radical polymerization (C/LRP) was initially used to describe a chain polymerization in which chain breaking reactions were absent [11,12]. In such an ideal system, after initiation is completed, chains only propagate and do not undergo transfer and termination. However, transfer and termination often occur in real system. Thus, living polymerization (LP, no chain breaking reactions) and controlled polymerization (CP, formation of well defined polymers) are two separate terms.

A controlled polymerization can be defined as a synthetic method for preparing polymers with predetermined molecular weights, low polydispersity and controlled functionality.

Transfer and termination are allowed in a controlled polymerization if their contribution is sufficiently reduced by the proper choice of the reaction conditions such that polymer structure is not affected. On the other hand, living polymerizations will lead to well defined polymers only if the following additional prerequisites are fulfilled:

- Initiation is fast in comparison with propagation
- Exchange between species of different reactivities is fast in comparison with propagation
- The rate of depropagation is low in comparison with propagation and the system is sufficiently homogeneous, in the sense of availability of active centers and mixing.

Well-defined polymers [13] may be formed in radical polymerization only if chains are relatively short and concentration of active center (free radicals) is low enough. There is apparent contradiction between these two requirements because usually a

decrease of the concentration of radicals leads to higher molecular weights. However, the two conditions can be accommodated in systems with reversible deactivation of growing radicals. The controlled polymerization requires a low proportion of deactivated chains, which can be achieved by keeping molecular weight sufficiently low. This necessitates a relatively high concentration of the initiator, or in other words, low  $[M]_0 / [I]_0$  ratios. However, when  $[I]_0$  is high, since the termination is bimolecular, contribution of termination becomes more significant when a large concentration of radicals  $[R^\bullet]$  is generated.

Therefore establishing an exchange between dormant and active species is necessary to solve this discrepancy. The concentration of dormant species can be equal to  $[I]_0$ , and the concentration of momentarily active species to  $[R^\bullet]$ . The total number of growing chains will be equal to  $[I]_0$ , and radicals would be present at a very low stationary concentration,  $[R^\bullet]$ , and therefore the contribution of termination should be very low.

The three approaches have been used to control radical systems. The best examples of the first approach include stable free radical polymerization (SFRP), atom transfer radical polymerization (ATRP), and reversible addition-fragmentation transfer polymerization (RAFT) based on photo labile iniferters. The second approach is less common and may be included some organometallic species such as Cr(III) or Al derivatives as well as nonpolymerizable alkenes such as stilbene or tetra thiafulvalene. The last approach can be best-exemplified chemistry, via methacrylate monomers [14].

### 2.3.2 Atom Transfer Radical Polymerization (ATRP)

ATRP is one of the most versatile controlled radical polymerization method [15,16]. This method utilizes a reversible halogen atom abstraction step in which a lower oxidation state metal complex ( $M_t^n$  complexed by ligand) reacts with an alkyl halide (R-X) to generate a radical ( $R^\bullet$ ), with an activation rate constant ( $k_a$ ), and a higher oxidation state metal complex ( $X-M_t^{n+1}/Ligand$ ). This radical then adds monomer to generate the polymer chain ( $k_p$ ). The higher oxidation state metal can then deactivate the growing radical to generate a dormant chain and the lower oxidation state metal complex ( $k_d$ ) as seen in Figure 2.11. The molecular weight is controlled because both initiation and deactivation are fast, allowing for all the chains to begin growing at approximately the same time while maintaining a low concentration of active

species. Termination cannot be totally avoided; however, the proportion of chains terminated compared to the number of propagating chains is small [17]. Several metal/ligand systems have been used to catalyze this process and a variety of monomers including styrene, (meth)acrylates, and acrylonitrile have been successfully polymerized [18-20].

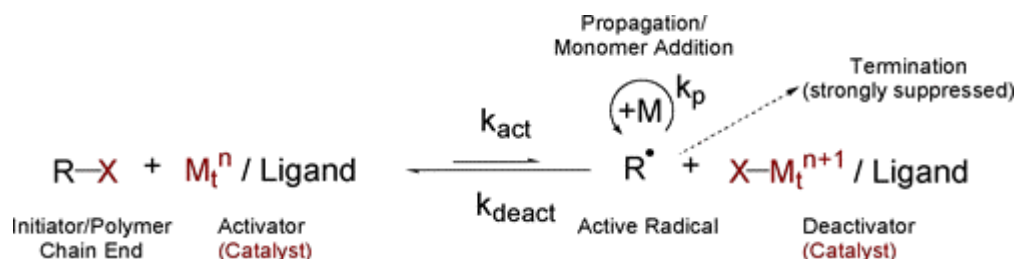


**Figure 2.11.** Transition Metal Catalyzed ATRP

The rate of ATRP is internally first order in monomer, externally first order with respect to initiator and activator,  $\text{M}_t^n$ , and negative first order with respect to deactivator,  $\text{X-M}_t^{n+1}$ . The actual kinetics depends on many factors including the solubility of activator and deactivator, their possible interactions, and variation of their structures and reactivities with concentrations and composition of the reaction medium.

One of the most important parameters in ATRP is the dynamics of exchange, especially the relative rate of deactivation. If the deactivation process is slow in comparison with propagation, then a classic redox initiation process operates leading to conventional, and not controlled, radical polymerization. Polydispersities in ATRP decrease with conversion, with the rate constant of deactivation,  $k_d$ , and also with the concentration of deactivator,  $[\text{X-M}_t^{n+1}]$ . They, however, increase with the propagation rate constant,  $k_p$ , and the concentration of initiator,  $[\text{R-X}]_0$ . This means that more uniform polymers are obtained at higher conversion, when the concentration of deactivator in solution is high and the concentration of initiator is low. Also, more uniform polymers are formed when deactivator is very reactive and monomer propagates slowly (styrene rather than acrylate) [21].

The product of an ATRP reaction is a potential initiator for yet another reaction, as it still has the halogen moiety in the growing chain end, which allows reactivation of the chain end using the initially synthesized polymer as macroinitiator for a second polymerization reaction either by sequential addition or reinitiation. Industrially produced polymers have also been functionalized and used as macroinitiators for

ATRP. A number of different polymer architectures have been synthesized by ATRP including star-shaped, graft and dendritic polymers.

### 2.3.2.1 Monomers

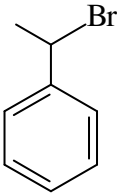
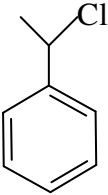
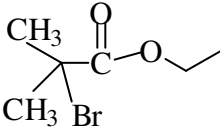
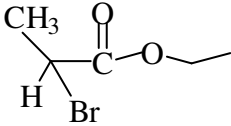
A variety of monomers have been successfully polymerized using ATRP. Typical monomers include styrenes, (meth)acrylates, (meth)acrylamides, and acrylonitrile, which contain substituents that can stabilize the propagating radicals. Even under the same conditions using the same catalyst, each monomer has its own unique atom transfer equilibrium constant for its active and dormant species. In the absence of any side reactions other than radical termination by coupling or disproportionation, the magnitude of the equilibrium constant ( $K_{eq}=k_a/k_d$ ) determines the polymerization rate.

### 2.3.2.2 Initiators

The main role of the initiator is to determine the number of growing polymer chains. Two parameters are important for a successful ATRP initiating system. First, initiation should be fast in comparison with propagation. Second, the probability of the side reactions should be minimized.

Initiators for ATRP must have a halogen (Br or Cl) and a functional group that can stabilize the formed radical, e.g. carbonyl, cyano or phenyl. The initiator is normally chosen so that the structure mimics the structure of the monomer with the aim of making the rate of initiation and propagation equivalent ( $k_i = k_p$ ). Different functionalities can be incorporated in the initiator and a number of functional groups can be tolerated including epoxide, hydroxyl, cyano and lactones. Multifunctional initiators can be used to synthesize more advanced structures such as star, graft polymers. [21] In ATRP, alkyl halides (R-X) are typically used as initiator (Table 2.2) and the rate of polymerization is first order with respect to the concentration of R-X. To obtain well-defined polymers with narrow molecular weight distributions, the halide group, X, must rapidly and selectively migrate between the growing chain and the transition metal complex. When X is either bromine or chlorine, the molecular weight control is the best. Fluorine is not used because the C-F bond is too strong to undergo homolytic cleavage.

**Table 2.2.** The Most Frequently Used Initiator Types in ATRP Systems

Initiator	Monomer
 1-Bromo-1-phenyl ethane	Styrene
 1-Chloro-1-phenyl ethane	Styrene
 Ethyl-2-bromo isobutyrate	Methyl methacrylate
 Ethyl-2-bromo propionate	Methyl acrylate and Styrene

### 2.3.2.3 Ligands

Transition metal catalysts are the key to ATRP since they determine the position of the atom transfer equilibrium and the dynamics of exchange between the dormant and active species. The main effect of the ligand is to solubilize the transition-metal salt in organic media and to regulate the proper reactivity and dynamic halogen exchange between the metal center and the dormant species or persistent radical. Ligands, typically amines or phosphines, are used to increase the solubility of the complex transition metal salts in the solution and to tune the reactivity of the metal towards halogen abstraction. So far, a range of multidentate neutral nitrogen ligands was developed as active and efficient complexing agents for copper-mediated ATRP, including, bipyridine [22-24] (Figure 2.13), terpyridines [25], phenantrolines[26], picolyl amines [25,26], pyridinemethinamines and tri [22] or tetradentate aliphatic amines [27] including linear and branched amines. Tridentate and tetradentate ligands generally provide faster polymerizations than bidentate ligands, while

monodentate nitrogen ligands yield redox-initiated free radical polymerization. In addition, ligands with an ethylene linkage between the nitrogens are more efficient than those with a propylene or butylene linkage [28].

Linear amines with ethylene linkage like tetramethylethylenediamine (TMEDA), 1,1,4,7,7-pentamethyldiethylenetriamine (PMDETA) and 1,1,4,7,10,10-hexamethyltriethylenetetramine (HMTETA) (Figure 2.12) were synthesized and examined for ATRP as ligands [43]. Reasons for examining of these type of ligands are, they have low price, due to the absence of the extensive  $\pi$ -bonding in the simple amines, the subsequent copper complexes are less colored and since the coordination complexes between copper and simple amines tend to have lower redox potentials than the copper-bpy complex, the employment of simple amines as the ligand in ATRP may lead to faster polymerization rates. The most widely used ligands for ATRP systems are the derivatives of 2,2-bipyridine and nitrogen based ligands such as

- N,N,N',N'',N'''-pentamethyldiethylenetriamine (PMDETA),
- Tetramethylethylenediamine (TMEDA),
- 1,1,4,7,10,10-hexamethyltriethylenetetraamine (HMTETA),
- Tris[2-(dimethylamino) ethyl]amine (Me<sub>6</sub>-TREN)
- Alkylpyridylmethanimines are also used.

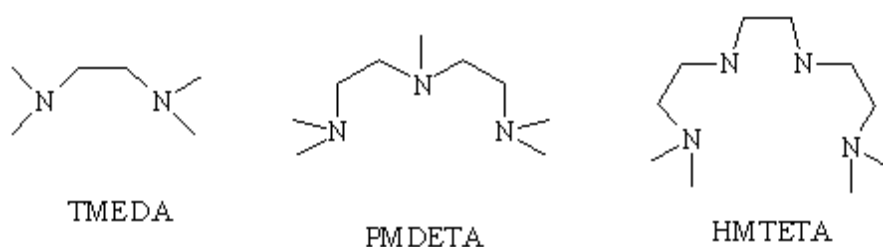


**Figure 2.12:** Nitrogen Based Ligands

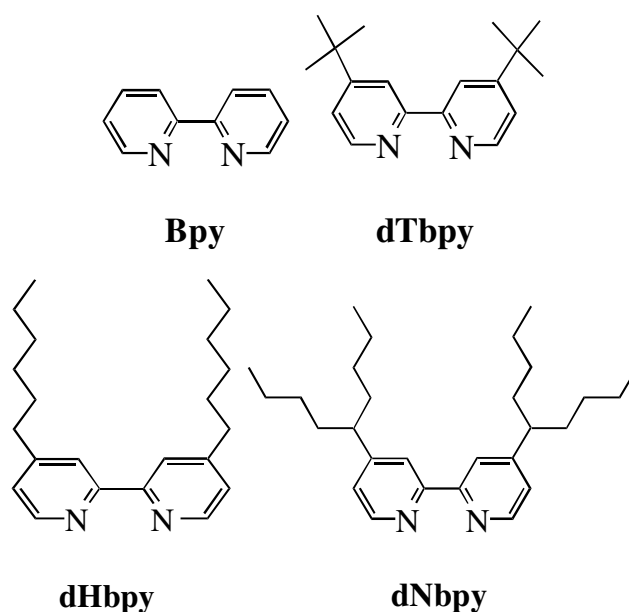


**Figure 2.13.** Derivatives of 2,2-Bipyridine

Solubility of the ligand and its metal complexes in organic media is of particular importance to attain homogeneous polymerization conditions. The rate of polymerization is also affected by the relative solubilities of the activating and the deactivating species of the catalyst. In heterogeneous systems, a low stationary concentration of the catalyst species allows for a controlled polymerization, but the polymerization is much slower than in homogeneous systems [28]. The ligand with a long aliphatic chain on the nitrogen atoms provides solubility of its metal complexes in organic solvents. However, the increasing length of the alkyl substituents induces steric effects and can alter the redox potential of the metal center. Any shift in the redox potential affects the electron transfer and the activation–deactivation equilibrium. [25]

#### 2.3.2.4 Transition Metal Complexes

Catalyst is the most important component of ATRP. It is the key to ATRP since it determines the position of the atom transfer equilibrium and the dynamics of exchange between the dormant and active species. There are several prerequisites for an efficient transition metal catalyst. First, the metal center must have at least two readily accessible oxidation states separated by one electron. Second the metal center should have reasonable affinity toward a halogen and finally that it can complex strongly with the ligand. Third the coordination sphere around the metal should be expandable upon oxidation to selectively accommodate a (pseudo)-halogen. The

most important catalysts used in ATRP are; Cu(I)Cl, Cu(I)Br, NiBr<sub>2</sub>(PPh<sub>3</sub>)<sub>2</sub>, FeCl<sub>2</sub>(PPh<sub>3</sub>)<sub>2</sub>, RuCl<sub>2</sub>(PPh<sub>3</sub>)<sub>3</sub>/ Al(OR)<sub>3</sub>.

### 2.3.2.5 Solvents

ATRP can be carried out either in bulk, in solution or in a heterogeneous system (e.g. emulsion, suspension). Various solvents such as benzene, toluene, anisole, diphenyl ether, ethyl acetate, acetone, dimethyl formamide (DMF), ethylene carbonate, alcohol, water, carbon dioxide and many others have been used for different monomers which has attracted attention because of environmental friendliness and cost reduction. A solvent is sometimes necessary especially when the obtained polymer is insoluble in its monomer.

### 2.3.2.6 Temperature and Reaction Time

The rate of polymerization also determines the rate of polymerization by effecting both propagation rate constant and the atom transfer equilibrium constant. The  $k_p/k_t$  ratio increase as a result of higher temperature thus enables us better control over the polymerization. However this may also increase the side reactions and chain transfer reactions. The increasing temperature also increases the solubility of the catalyst. Against this, it may also poison catalyst by decomposition. Determining the optimum temperature; monomer, catalyst and the targeted molecular weight should be taken into consideration.

### 2.3.2.7 Kinetics of ATRP

The rate of polymerization is first order with respect to monomer, alkyl halide (initiator), and transition metal complexed by ligand. The reaction is usually negative first order with respect to the deactivator ( $X-M_t^{n+1}/Ligand$ ).

The rate equation of copper-based ATRP is formulated in discussed conditions and given in figure 2.14.

$$R_p = k_{app} [M] = k_p [R\cdot] [M] = k_p K_{eq} [M] [I]_0 ([CuX]/[CuX_2])$$

**Figure 2.14.** The Rate Equation of Copper-Based ATRP

Figure 2.14 shows a typical linear variation of conversion with time in semi logarithmic coordinates (kinetic plot). Such a behavior indicates that there is a constant concentration of active species in the polymerization and first-order kinetics with respect to monomer. However, since termination occurs continuously, the concentration of the Cu(II) species increases and deviation from linearity may be observed [13]. For the ideal case with chain length independent from termination, persistent radical effect kinetics implies the semi logarithmic plot of monomer conversion vs. time to the 2/3 exponents should be linear. Nevertheless, a linear semi logarithmic plot is often observed. This may be due to an excess of the Cu(II) species present initially, a chain length dependent termination rate coefficient, and heterogeneity of the reaction system due to limited solubility of the copper complexes. It is also possible that self-initiation may continuously produce radicals and compensate for termination. Similarly, external orders with respect to initiator and the Cu(I) species may also be affected by the persistent radical effect [29].

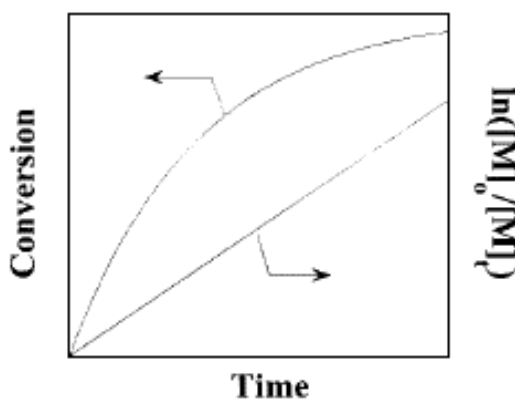


**Figure 2.15.** Kinetic Plot and Conversion vs. Time Plot for ATRP

Results from kinetic studies of ATRP for styrene (St) [30], methyl acrylate (MA) [31] and methyl methacrylate (MMA) [25,31] under homogeneous conditions indicate that the rate of polymerization is first order with respect to monomer, initiator, and Cu(I) complex concentrations. These observations are all consistent with the derived rate law.

It should be noted that the optimum ratio could vary with regard to changes in the monomer, counter ion, ligand, temperature, and other factors [24]. The precise kinetic law for the deactivator  $\text{CuX}_2$  was more complex due to the spontaneous generation of Cu(II) via the persistent radical effect [29-30]. In the atom transfer

step, a reactive organic radical is generated along with a stable Cu(II) species that can be regarded as a persistent metallo-radical. If the initial concentration of deactivator Cu(II) in the polymerization is not sufficiently large to ensure a fast rate of deactivation ( $k_d[\text{Cu(II)}]$ ), then coupling of the organic radicals will occur, leading to an increase in the Cu(II) concentration.

Radical termination occurs rapidly until a sufficient amount of deactivator Cu(II) is formed and the radical concentration becomes low enough. Under such conditions, the rate at which radicals combine ( $k_t$ ) will become much slower than the rate at which radicals react with the Cu(II) complex in a deactivation process and a controlled polymerization will proceed. Typically, a small fraction (~5 %) of the total growing polymer chains will be terminated during the early stage of the polymerization, but the majority of the chains (>95 %) will continue to grow successfully. The effect of Cu(II) on the polymerization may additionally be complicated by its poor solubility, by a slow reduction by reaction with monomers leading to 1,2-dihaloadducts, or from the self-initiated systems such as styrene and other monomers. If the deactivation does not occur, or if it is too slow ( $k_p \gg k_d$ ), there will be no control and polymerization will become a classical redox reaction therefore the termination and transfer reactions may be observed. To gain better control over the polymerization, addition of one or a few monomers to the growing chain in each activation step is desirable. Molecular weight distribution for ATRP is given in equation 2.1.

$$M_w/M_n = 1 + ((k_d[\text{RX}]_0)/(k_p[\text{X-M}_t^{n+1}])) \times ((2/p)-1) \quad (2.1)$$

$p$  = polymerization yield  
 $[\text{RX}]_0$  = concentration of the functional polymer chain  
 $[\text{X-M}_t^{n+1}]$  = concentration of the deactivators  
 $k_d$  = rate constant of deactivation  
 $k_p$  = rate constant of polymerization

When a hundred percent of conversion is reached, in other words  $p=1$ , it can be concluded that;

a) For the smaller polymer chains, higher polydispersities are expected to be obtained because the smaller chains include little activation-deactivation steps and also the chain length difference is higher for small polymer chains resulting in little control of the polymerization.

b) For the higher ratios of  $k_p/k_d$ , higher polydispersities (molecular weight distributions) are usually obtained resulting in the little control of polymerization.

c) Resulting molecular weight distribution decreases as the concentration of the deactivators increases.

A number of functional groups are not tolerated in ATRP including carboxylic acid and certain ionic groups, which react with the catalyst, thereby impeding the establishment of the equilibrium. However, carboxylic acid groups can be introduced by polymerization of the carboxylic acid salt instead. Other monomers cannot be polymerized by this method, because the formed radical is not stabilized enough, which is the case for monomers such as vinyl acetate and halogenated alkenes. The main problem in using ATRP for syntheses, industrial or otherwise, is removal of the catalyst. The metal catalyst–ligand complex is undesired in the product, as the transition metal induces aging in the polymer, but also for aesthetic (coloration) and toxicological reasons removal is important. Catalyst removal is both difficult and costly, but several methods are presently in use. One procedure is to immobilize the catalyst by having it attached to solid supports during reaction, but this can give loss of control, perhaps due to reduced mobility. Other purification methods include running the raw product on an alumina column, precipitation of polymer and use of an absorbant.

### **2.3.3 Activator Generated by Electron Transfer ATRP**

This initiation system starts with alkyl halides as initiators and transition metal complexes in their oxidatively stable state as catalyst precursors. Therefore the most active catalyst complexes can be added to the reaction in their stable state. However, instead of employing a conventional radical initiator to activate the catalyst complex as in "reverse" ATRP, a non-radical forming reducing agent is employed to generate the activator. Reducing agents such as tin-2-ethylhexanoate [32], ascorbic acid [33], or MAO [34] react with the oxidatively stable Cu(II) complex and generate the activator, the transition metal complex in its lower oxidation state.

The activators are generated by electron transfer without involvement of organic radicals capable of initiating a radical reaction. Therefore an additional requirement for a successful AGET-ATRP is that the reducing agents should be selected so that the reduction occurs without formation of intermediates or products that could form





**Figure 2.17.** The Ford Focus FCV is Ford's Most Recent Hydrogen Car.

Several types of fuel cells exist [37-40], normally classified according to the type of electrolyte used, e.g. Solid Oxide Fuel Cell (SOFC), Molten Carbonate Fuel Cell (MCFC), Phosphoric Acid Fuel Cells (PAFC) and the Proton Exchangeable Membrane Fuel Cell (PEMFC). The operating temperature of the fuel cells is connected to the electrolyte used [1]. Through all types of fuel cells, PEMFC deliver the highest power density, which offers low weight, cost, and volume.

PEMFC converts hydrogen and oxygen electrochemically into electrical power, heat and water. It typically consists of an ion-conducting polymer membrane sandwiched between the anode and cathode, each containing a macroporous diffusion backing and an active catalyst layer (Figure 2.18). The role of a polymer membrane is to provide ionic conductivity, to prevent the flow of electrons, to act as a barrier to the reactants, and to maintain chemical and mechanical stabilities.

In a typical PEMFC, hydrogen is split into protons and electrons at the anode (negative electrode). The proton exchange membrane placed in the center allows protons to pass from the anode (negative electrode) to the cathode (positive electrode), while the electrons induce a current through an external circuit to the cathode. At the cathode, the electrons recombine with the protons that have crossed the membrane and with oxygen from the air. As long as fuel is supplied to the cell along with an oxidant, the fuel cell continues to produce electrical energy and heat. The only by-product when fueled with hydrogen is water.

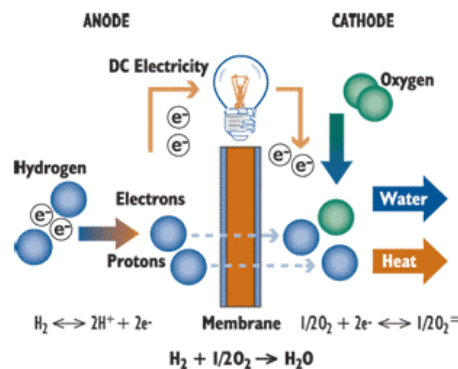


**Figure 2.18.** Schematic Representation of a Typical PEMFC

The most investigated proton exchange membranes (PEM) are based on fluorinated polymers, and, in particular, the DuPont Nafion 117. The reported chemical structure of Nafion for PEM membranes is shown in Figure 2.19.

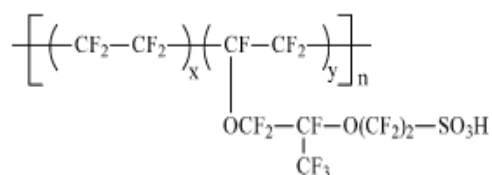


**Figure 2.19.** Structure of Nafion-117

In composite structures, Nafion can be impregnated into an inert Teflon-like matrix (i.e. W.L. Gore membranes)[44], or inorganic additives can be added to a supporting Nafion matrix for improved physical or electrochemical properties. By a suitable choice of alkyl groups, (e.g.  $-\text{COOH}$ ,  $-\text{PO}_3\text{H}$ ,  $-\text{SO}_3\text{H}$ ,  $-\text{NH}_3^+$ ), these compounds are proton conductors, the proton conductivity can be increased almost continuously to values as high as  $0.05 \text{ S cm}^{-1}$  which are comparable with Nafion membranes.

Nafion is a free radical initiated copolymer of a crystallizable hydrophobic tetrafluoroethylene (TFE) backbone sequence (87 mol % at 1100 equivalent weight) with a comonomer, which ultimately has pendant side chains of perfluorinated vinyl ethers terminated by perfluorosulfonic acid groups.

In theory, ion content can vary by changing the ratio of the two components ( $x$  and  $y$  in Figure 2.19). Nafion has been commercially available in 900, 1100, 1200, and other equivalent Nafion 1100 EW in thickness of 2, 5, 7, and 10 mil (1 mil equals 25.4  $\mu\text{m}$ ) (Nafion 112, 115, 117, and 1110) seems to be the only grades of Nafion that are currently widely available. This equivalent weight provides high protonic

conductivity and moderate swelling in water, which seems to suit most current applications and research efforts. Modest retention of semicrystalline morphology at this composition is no doubt important for mechanical strength. The thinner membranes are generally applied to hydrogen/ air applications to minimize Ohmic losses; Nafion is prepared via the copolymerization of variable amounts of the unsaturated perfluoroalkyl sulfonyl fluoride with tetrafluoroethylene. [42,43]

Unfortunately, there have been no detailed literature reports of Nafion's synthesis and processing, but it is generally thought that the copolymer is then extruded in the melt process able sulfonyl fluoride precursor to form a membrane, which is later converted from the sulfonyl fluoride form by base hydrolysis to the salt or sulfonic acid functionality. It seems unlikely that the sulfonyl fluoride containing precursor unit in the copolymer would self-propagate under free radical conditions. Thus, the length of the comonomer sequence ( $y$ ) is likely only one unit. Total molecular weight, though obviously important, has not been reported. Like many other fluoropolymers, Nafion is quite resistant to chemical attack, but the presence of its strong perfluorosulfonic acid groups imparts many of its desirable properties as a proton exchange membrane. Fine dispersions (sometimes incorrectly called solutions) can be generated with alcohol/water treatments. [41] Such dispersions are often critical for the generation of the catalyst electrode structure and the MEAs. Films prepared by simply drying these dispersions are often called "recast" Nafion, and it is often not realized that its morphology and physical behavior are much different from those of the extruded, more crystalline form.

The other known commercial membranes used today in numerous industrial processes throughout the World are Flemion<sup>®</sup> and Aciplex<sup>®</sup>, which were produced by DuPont ve Asahi. The basic common properties of this material are PTFE based backbone, fluorinated etheric side chain connecting the backbone to the third region of ionizable sulfonic or carboxylic acid end groups. As the fluorinated backbone possesses the chemical, mechanical and thermal resistivity to the molecule, the ionizable end groups at the side chain has high proton permeability and cation transfer capacity properties. The limitations to large-scale commercial use include poor ionic conductivities at low humidities and/or elevated temperatures, a susceptibility to chemical degradation at elevated temperatures and finally, membrane cost. Researchers around the world are seeking other polymer systems that would have even better performance than Nafion and/or have lower costs.

In order to overcome the limitations, many other alternative polymers have been tested during these years. The partially fluorinated polymer PVDF based proton exchange membranes seem to offer the most promising performances, combining high room temperature proton conductivity, chemical stability, good mechanical properties [37,40] and it is considerably cheaper than a fully fluorinated polymers.

The chemical modification by irradiation, ozonation or direct initiation of PVDF followed by grafting of proton-exchange monomers or PS (post-functionalizable into sulfonic acid PS). The obtained copolymers seem to suffer from oxidizing decomposition, concomitant to the thermal degradation. Although some conductivity values seemed interesting, the presence or absence of the oxygen atom as a link between the polymeric backbone and the grafts is sometimes not mentioned. In addition, the chemical modification needs a special, heavy and expensive equipment to enable the irradiation or ozonation and the industrial production is probably difficult to achieve.

However, the development of fluorinated materials for electrolytes for fuel cells requires the synthesis of original functional fluorinated monomers to obtain new polymers and to optimize the characteristics of existing polymers in terms of molecular weight, crosslinking, new functional groups formation of hybrid or composite membranes or those made of multilayers.

### 3. EXPERIMENTAL PART

#### 3.1 Chemicals

N,N,N',N'',N'''-Pentamethyldiethylenetriamine (PMDETA, 99 %), *tert*-butyl acrylate (*t*BA, 99 %), trifluoroacetic acid (TFA, 99%), triethylamine (Et<sub>3</sub>N, 98 %), styrene (S, 99 %), 2-hydroxy ethyl acrylate (HEA, 97 %) were purchased from Across Organics Co., tetrahydrofuran (THF), acetone, chloroform (CHCl<sub>3</sub>), methanol (MeOH), dichloromethane (CH<sub>2</sub>Cl<sub>2</sub>) were purchased from J.T. Baker Co., copper (I) chloride (CuCl, 99.99 %), copper (II) chloride (CuCl<sub>2</sub>, 99.99 %) was purchased from Merck, 2-hydroxy ethyl methacrylate (HEMA, 97 %), 3-sulfo propyl methacrylate, potassium salt (SPMAP, 98 %), polyvinylidene fluoride (107K g mol<sup>-1</sup>, PVDF-107), dimethylformamid (DMF, Labscan, 99.8 %), N-Methyl-2-pyrrolidone (NMP, 99.5 %), 2-acrylamido-2-methyl-propansulfonic acid (AMPS, 99 %), ethylene glycdyl methacrylate phosphate (EGMAP), ethylene diamine (EDA) were purchased from Aldrich. All reagents were used without further purification. Vinyl phosphoric acid (VPA, 90 %), was purchased from Clariant, glycdyl methacrylate (GMA, 95%) was purchased from Alfa Aesar GmbH. Diethyl ether (technical grade). Tris [2-(dimethylamino) ethyl] amine (Me<sub>6</sub>-TREN) was synthesized according to literature [9,45].

Table 3.1 presents the monomers that are used to synthesise graft copolymers of PVDF by ATRP and AGET- ATRP.

**Table 3.1.** Monomers Used in PVDF-Based Graft Copolymerization

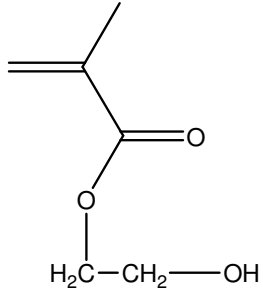
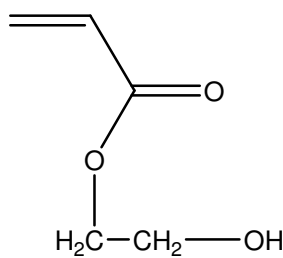
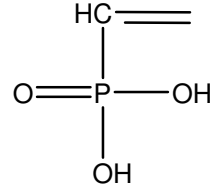
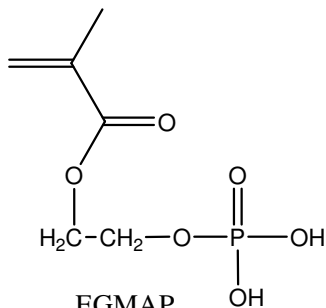
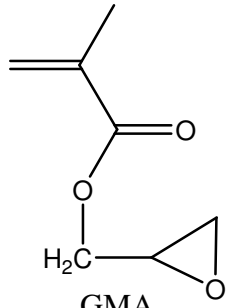
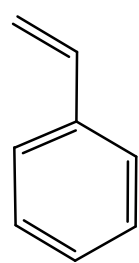
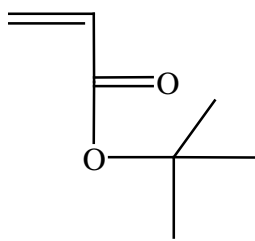
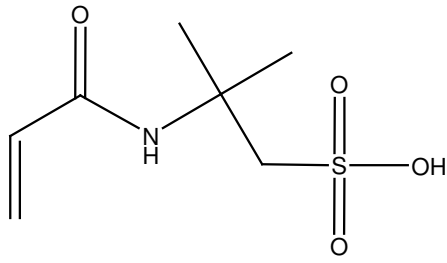
 <p>HEMA</p>	 <p>HEA</p>	 <p>VPA</p>
 <p>EGMAP</p>	 <p>GMA</p>	 <p>S</p>
 <p>tBA</p>	 <p>AMPS</p>	

Table 3.2 presents monomers that are containing ionic functionality synthesized by hydrolysis reaction to synthesise PVDF-based graft copolymers by ATRP and AGET- ATRP.

**Table 3.2** Modified Monomers Used in PVDF-Based Graft Copolymerization

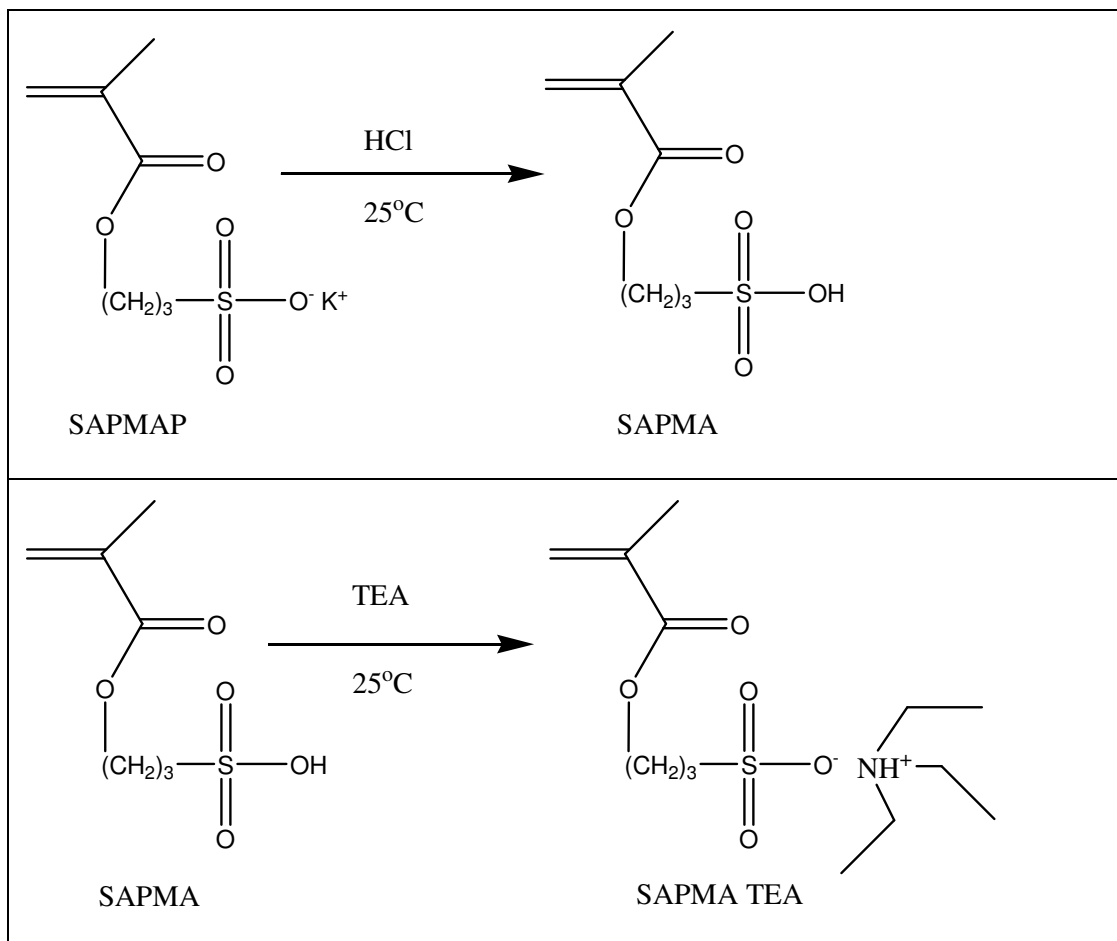
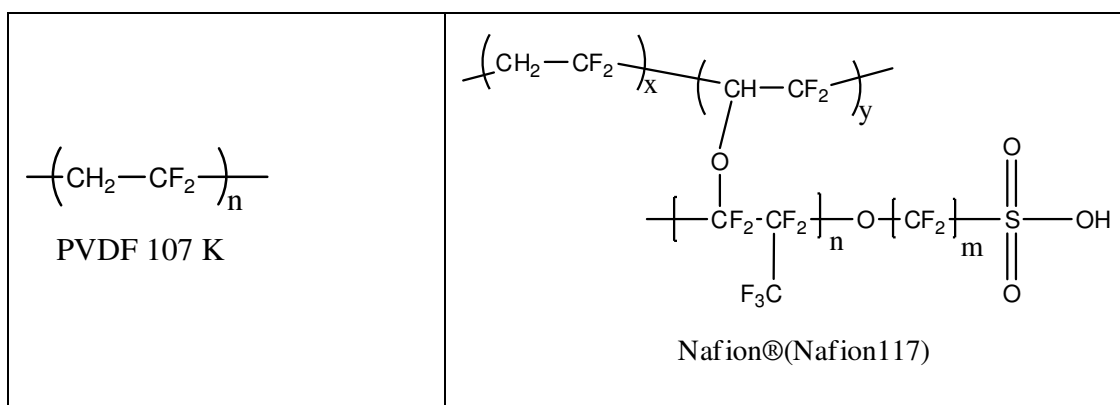


Table 3.3 presents PVDF homopolymer that has a molecular weight of 107K.

**Table 3.3.** PVDF as Macroinitiator and Its Commercial Structure, Nafion-117



## 3.2 PVDF Based Graft Copolymerization by AtomTransfer Radical Polymerization (ATRP)

### 3.2.1 Synthesis of PVDF-g-PAA Graft Copolymer

ATRP procedure was performed as follows; catalyst, CuCl (0.01 g,  $1 \times 10^{-4}$  mol), was placed in a 48 ml of flask, which contained a side arm with a Teflon valve sealed with a Teflon stopper. Then the flask was deoxygenated three times by vacuum-nitrogen cycles, macroinitiator PVDF-107(0.5 g,  $4.67 \times 10^{-6}$  mol) priority dissolved in 5 ml of DMF at 50 °C and *t*BA (0.5 g,  $3.9 \times 10^{-3}$  mol) were added to the flask, respectively. Finally, nitrogen bubbled ligand PMDETA (0.02 g,  $1.2 \times 10^{-4}$  mol) was added into the flask. Then the mixture was nitrogen bubbled for 30 minutes before the flask was replaced in thermostatically controlled oil bath at 90 °C at 500 rpm stirring rate to initiate the graft copolymerization. [Monomer]:[initiator]:[catalyst]:[ligand] ratio was 835:1:21.4:26 for PVDF-*g*-*Pt*BA copolymerization. After 24 h reaction time, the reaction flask was cooled and PVDF-*g*-*Pt*BA graft copolymer was precipitated in excess of cold methanol/water solvent mixture and filtered. After filtration, polymer was dried for 24 h in a vacuum oven at 50 °C. PVDF-*g*-*Pt*BA graft copolymer was further purified by stirring for 24 h in an excess amount of THF at room temperature remove the residual *Pt*BA homopolymer, if any. Dissolved PVDF-*g*-*Pt*BuA graft copolymer was precipitated in cold methanol distilled water solvent mixture again, filtered and dried in a vacuum oven at 50 °C.

Then, obtained PVDF-*g*-*Pt*BA graft copolymer in THF was replaced in CHCl<sub>3</sub> (5 ml) and TFA (3ml) was slowly added into the polymer/solvent mixture under stirring at room temperature. Finally, PVDF-*g*-PAA graft copolymer was precipitated in cold excess methanol/water solvent mixture. Then PVDF-*g*-PAA graft copolymer was filtered and dried in a vacuum oven at 50 °C.

### 3.2.2 Synthesis of PVDF-*g*-PSPMAP Graft Copolymer

ATRP procedure was performed as follows; catalyst, CuCl (0.01 g,  $1 \times 10^{-4}$  mol), was placed in a 100 ml of flask, which contained a side arm with a Teflon valve sealed with a Teflon stopper. Then the flask was deoxygenated three times by vacuum-nitrogen cycles, macroinitiator PVDF-107 (0.5 g,  $4.67 \times 10^{-6}$  mol) priority dissolved in 5 ml of DMF at 50 °C, PSPMAP (2.5 g,  $1.02 \times 10^{-2}$  mol) and DMF (40

ml) were added to the flask, respectively. Finally, nitrogen bubbled ligand PMDETA (0.02 g,  $1.2 \times 10^{-4}$  mol) was added into the flask. Then the mixture was nitrogen bubbled before the flask was replaced in thermostatically controlled oil bath at 100 °C at 700 rpm stirring rate to initiate the graft copolymerization. [Monomer]:[initiator]:[catalyst]:[ligand] ratio was 2184:1:21.4:26 for PVDF-*g*-PSPMAP copolymerization. After 22 days, the reaction flask was cooled and PVDF-*g*-PSPMAP graft copolymer was precipitated in diethyl ether and filtered. After filtration, polymer was dried for 24 h in a vacuum oven at 50 °C. PVDF-*g*-PSPMAP graft copolymer was further purified by stirring for 24 h in an excess amount of water at 100 °C to remove the residual PSPMAP homopolymer and to test the solubility ratio of PVDF-*g*-PSPMAP graft copolymer at 100 °C boiling water. Purified PVDF-*g*-PSPMAP graft copolymer was filtered and dried in a vacuum oven at 50 °C. PVDF-*g*-PSPMAP graft copolymer was placed in a 100 ml of flask, which contained 50 ml of CH<sub>2</sub>Cl<sub>2</sub>. Then HCl (4 ml) was added drop wise to the flask by stirring at 700 rpm at room temperature. After 4 days, the CH<sub>2</sub>Cl<sub>2</sub> was evaporated and remaining polymer, PVDF-*g*-PSAPMA was dried in a vacuum oven at 50 °C.

### 3.2.3 Synthesis of PVDF-*g*-PSAPMA-TEA Graft Copolymer

SPMAP (1.25 g,  $0.51 \times 10^{-2}$  mol) monomer was dissolved in DMF (22.5 ml) and TFA (1.75 g,  $1.53 \times 10^{-2}$  mol) was added slowly under stirring at room temperature into the monomer/DMF solution to synthesize SAPMA monomer. Then TEA (2.06 g, 2.85 ml,  $2.04 \times 10^{-2}$  mol) was added slowly under stirring at room temperature into the SAPMA monomer in DMF solution. The SAPMA monomer solution was stirred for 48 h to synthesize SAPMA-TEA salt.

Finally, ATRP procedure was performed as follows; catalyst, CuCl (0.01 g,  $1 \times 10^{-4}$  mol) was placed in a 100 ml of flask, which contained a side arm with a Teflon valve sealed with a Teflon stopper. Then the flask was deoxygenated three times by vacuum-nitrogen cycles, macroinitiator PVDF-107 (0.25 g,  $2.34 \times 10^{-6}$  mol) priority dissolved in 2.5 ml of DMF at 50 °C, the DMF solution of SAPMA-TEA monomer (1.25 g SAPMA, 22.5 ml DMF, 2.06 g TEA) and ligand PMDETA (0.86 g,  $5 \times 10^{-3}$  mol) priority nitrogen bubbled were added to the flask, respectively. Then mixture was nitrogen bubbled before the flask was replaced in thermostatically controlled oil bath

at 100 °C at 700 rpm stirring rate to initiate the graft copolymerization. After 18 day the reaction flask was cooled and PVDF-*g*-PSAPMA-TEA graft copolymer was precipitated in diethyl ether and filtered. After filtration, polymer was dried for 24 h in a vacuum oven at 50 °C.

PVDF-*g*-PSAPMA-TEA graft copolymer was further purified by desired time in an excess amount of water at 100 °C to remove the residual PSAPMA-TEA homopolymer and to test the solubility ratio of PVDF-*g*-PSAPMA-TEA graft copolymer at 100 °C boiling water. Precipitant, PVDF-*g*-PSAPMA-TEA graft copolymer was filtered and dried in a vacuum oven at 50 °C.

### **3.2.4 Synthesis of PVDF-*g*-PHEMA Graft Copolymer**

ATRP procedure was performed as follows; catalyst, CuCl (0.4 g,  $4 \times 10^{-3}$  mol), was placed in a 250 ml of flask, which contained a side arm with a Teflon valve sealed with a Teflon stopper. Then the flask was deoxygenated three times by vacuum-nitrogen cycles, macroinitiator PVDF-107 (2 g,  $1.87 \times 10^{-5}$  mol) priority dissolved in 40 ml of DMF at 50 °C, HEMA (4.06 g,  $3.12 \times 10^{-2}$  mol) and solvent DMF (20 ml) were added to the flask, respectively. Finally, nitrogen bubbled ligand PMDETA (0.27 g,  $1.56 \times 10^{-3}$  mol) was added. Then mixture were nitrogen bubbled before the flask was replaced in thermostatically controlled oil bath at 80 °C at 500 rpm stirring rate to initiate the graft copolymerization. [Monomer]:[initiator]:[catalyst]:[ligand] was 1670:1:83:83 for PVDF-*g*-PHEMA copolymerization. After 3 days reaction time, the reaction flask was cooled and PVDF-*g*-PHEMA graft copolymer was precipitated in excess of cold methanol/water mixture, filtered and dried in a vacuum oven at 50 °C. PVDF-*g*-PHEMA graft copolymer was further purified by stirring for 24 h in an excess amount of water at room temperature to remove the residual PHEMA homopolymer and to determine the solubility ratio of PVDF-*g*-PHEMA graft copolymer in water. Precipitant, PVDF-*g*-PHEMA graft copolymer was filtered and dried in a vacuum oven at 50 °C.

### **3.2.5 Synthesis of PVDF-*g*-PHEA Graft Copolymer**

ATRP procedure was performed as follows; catalyst, CuCl (0.05 g,  $6 \times 10^{-4}$  mol) was placed in a 100 ml of flask, which contained a side arm with a Teflon valve sealed

with a Teflon stopper. Then the flask was deoxygenated three times by vacuum-nitrogen cycles, macroinitiator PVDF-107 (2 g,  $1.87 \times 10^{-5}$  mol) priority dissolved in 20 ml of DMF at 80 °C, HEA (2 g,  $1.7 \times 10^{-2}$  mol), and 20 ml of DMF were added to the flask respectively and the mixture was nitrogen bubbled for 30 min. Finally ligand Me<sub>6</sub>-TREN (0.21 g,  $9 \times 10^{-4}$  mol) was added to the flask, then the mixture was nitrogen bubbled again for 5 min before the flask was replaced in thermostatically controlled oil bath at 100 °C at 400 rpm to initiate the graft copolymerization. [Monomer]:[initiator]:[catalyst]:[ligand] ratio was 921:1.32:48 for PVDF-*g*-PHEA copolymerization. After 31 days reaction time, the reaction flask was cooled and PVDF-*g*-PHEA graft copolymer was precipitated in excess of water. Then copolymer was filtered and dried in a vacuum oven at 50 °C. PVDF-*g*-PHEA graft copolymer was further purified by stirring for 24 h in an excess amount of THF at room temperature to remove the residual PHEA homopolymer. Purified PVDF-*g*-PHEA graft copolymer was filtered and dried in a vacuum oven 50 °C.

### 3.2.6 Synthesis of PVDF-*g*-PAMPS Graft Copolymer

ATRP procedure was performed as follows; catalyst, CuBr (0.086 g,  $6 \times 10^{-4}$  mol), was placed in a 100 ml of flask, which contained a side arm with a Teflon valve sealed with a Teflon stopper. Then the flask was deoxygenated three times by vacuum-nitrogen cycles, macroinitiator PVDF-107 (2 g,  $1.87 \times 10^{-5}$  mol) priority dissolved in 20 ml of DMF at 80 °C, AMPS (0.5 g,  $2.5 \times 10^{-3}$  mol), 20 ml of DMF and ligand PMDETA (0.156 g,  $9 \times 10^{-4}$  mol) priority bubbled were added to the flask, respectively. Then the mixture was nitrogen bubbled before the flask was replaced in thermostatically controlled oil bath at 100°C at 400 rpm to initiate the graft copolymerization. [Monomer]:[initiator]:[catalyst]:[ligand] ratio was 134:1:32:48 for PVDF-*g*-PAMPS copolymerization. After the 11 days reaction time the reaction flask was cooled and PVDF-*g*-PAMPS graft copolymer was precipitated in excess diethyl ether. Then PVDF-*g*-PAMPS graft copolymer was filtered and dried in a vacuum oven at 50 °C.

### 3.2.7 Synthesis of PVDF-*g*-PVPA Graft Copolymer

ATRP procedure was performed as follows. Catalyst, CuCl (0.086 g,  $9.39 \times 10^{-4}$  mol), was placed in a 100 ml of flask, which contained a side arm with a Teflon

valve sealed with a Teflon stopper. Then the flask was deoxygenated three times by vacuum-nitrogen cycles, macroinitiator PVDF-107 (3 g,  $2.8 \times 10^{-5}$  mol) priority dissolved in 30 ml of DMF at 80 °C, VPA (0.8 g,  $7.7 \times 10^{-3}$  mol), DMF (20 ml), and ligand PMDETA (0.156 g,  $9.39 \times 10^{-4}$  mol) priority nitrogen bubbled was added to the flask respectively. Then all liquid components were nitrogen bubbled before the flask was replaced in thermostatically controlled oil bath at 90°C at 700 rpm stirring rate to initiate the graft copolymerization. [Monomer]:[initiator]:[catalyst]:[ligand] ratio was 275:1:33:33 for PVDF-*g*-PVPA copolymerization. After the 7 days reaction time the reaction flask was cooled and PVDF-*g*-PVPA graft copolymer was precipitated in excess diethyl ether Then PVDF-*g*-PVPA graft copolymer was filtered and dried in a vacuum oven at 50 °C.

### **3.2.8 Synthesis of PVDF-*g*-PGMA Graft Copolymer**

ATRP procedure was performed as follows. Catalyst, CuCl (0.05 g,  $6 \times 10^{-4}$  mol), was placed in a 100 ml of flask, which contained a side arm with a Teflon valve sealed with a Teflon stopper. Then the flask was deoxygenated three times by vacuum-nitrogen cycles, macroinitiator PVDF-107 (2 g,  $1.87 \times 10^{-5}$  mol) priority dissolved in 20 ml of DMF at 80 °C, GMA (2 g,  $1.4 \times 10^{-2}$  mol) and solvent DMF (20 ml) was added to the flask, respectively. The mixture was nitrogen bubbled for 30 min. Finally, ligand Me<sub>6</sub>-TREN (0.156 g,  $9 \times 10^{-4}$  mol) was added, then all liquid components were nitrogen bubbled again for 5 min. before the flask was replaced in thermostatically controlled oil bath at 100°C at 400 rpm stirring rate to initiate the graft copolymerization. [Monomer]:[initiator]:[catalyst]:[ligand] ratio was 748:1:32:48 for PVDF-*g*-PGMA copolymerization. After the 1 days reaction time the reaction flask was cooled and PVDF-*g*-PGMA graft copolymer was precipitated in excess diethyl ether. Then PVDF-*g*-PGMA graft copolymer was filtered and dried in a vacuum oven at 50 °C.

### **3.2.9 Synthesis of PVDF-*g*-PSA Graft Copolymer**

ATRP procedure was performed as follows. Catalyst, CuCl (0.04 g,  $4 \times 10^{-4}$  mol), was placed in a 250 ml of flask, which contained a side arm with a Teflon valve sealed with a Teflon stopper. Then the flask was deoxygenated three times by vacuum-nitrogen cycles, macroinitiator PVDF-107 (5 g,  $4.7 \times 10^{-5}$  mol) priority

dissolved in 100 ml of DMF at 80 °C, S (18 g,  $1,72 \times 10^{-1}$  mol) and solvent NMP (50 ml) were added to the flask, respectively, and the mixture was nitrogen bubbled for 30 min. Finally, ligand Me<sub>6</sub>-TREN (0.26 g,  $1,16 \times 10^{-3}$  mol) was added and all liquid components were nitrogen bubbled again for 5 min. before the flask was replaced in thermostatically controlled oil bath at 100°C at 500 rpm stirring rate to initiate the graft copolymerization. [Monomer]:[initiator]:[catalyst]:[ligand] ratio was 4255:1:8:25 for PVDF-*g*-PS copolymerization. After the 14 days reaction time the reaction flask was cooled and PVDF-*g*-PS graft copolymer was precipitated in excess water, filtered and dried in a vacuum oven at 50 °C. PVDF-*g*-PS graft copolymer was further purified by stirring for 24 h in an excess amount of THF at room temperature to remove the residual PS homopolymer if any. Purified PVDF-*g*-PS graft copolymer was filtered and dried in a vacuum oven at 50 °C.

To sulphonate PVDF-*g*-PS graft copolymer, firstly 0.5 M Chlorosulphonic acid (HSO<sub>3</sub>Cl) solution was prepared in dichloromethane (CH<sub>2</sub>Cl<sub>2</sub>). Chlorosulphonic acid solution was prepared by mixing a fixed amount of CH<sub>2</sub>Cl<sub>2</sub> (14 ml) and HSO<sub>3</sub>Cl (0,81 g,  $7 \times 10^{-3}$  mol, 0,46 ml). HSO<sub>3</sub>Cl was carefully added into the CH<sub>2</sub>Cl<sub>2</sub> solvent. This reaction mixture was stirred under heterogeneous conditions at room temperature. The HSO<sub>3</sub>Cl solution was freshly prepared prior to each sulfonation reaction.

PVDF-*g*-PS (3,6 g,  $7 \times 10^{-3}$  mol) was placed in a 50 ml of flask round-bottomed. A freshly prepared HSO<sub>3</sub>Cl solution was added carefully using the separator funnel. The reaction mixture was maintained at 25 °C under stirring for 96 h. After 96 hours reaction time the reaction mixture was filtered. PVDF-*g*-PSA graft copolymer was washed with excess amount of water and THF respectively. Finally sulfonated copolymer was dried in a vacuum oven at 50 °C after drying it was kept in a desiccator for characterizing.

### **3.3 PVDF Based Graft Copolymerization with Activators Generated by Electron Transfer (AGET) ATRP**

#### **3.3.1 Synthesis of PVDF-*g*-PSPMAP Graft Copolymer**

AGET-ATRP procedure was performed as follows: catalyst, CuCl<sub>2</sub> (0.08 g, 6 x 10<sup>-4</sup> mol) and as reducing agent ascorbic acid (1.04 g, 6 x 10<sup>-3</sup> mol), was placed in a 100 ml of flask, which contained a side arm with a Teflon valve sealed with a Teflon stopper. Then the flask was deoxygenated three times by vacuum-nitrogen cycles, macroinitiator PVDF-107 (2 g, 1.87 x 10<sup>-5</sup> mol) priority dissolved in 40 ml of NMP at 80 °C, PSPMAP (2 g, 8 x 10<sup>-3</sup> mol) were added to the flask, respectively, and the mixture was nitrogen bubbled for 30 min. Finally, ligand Me<sub>6</sub>-TREN (0.21 g, 9 x 10<sup>-4</sup> mol) was added, then all liquid components were nitrogen bubbled again for 5 min before the flask was replaced in thermostatically controlled oil bath at 100°C at 400 rpm stirring rate to initiate the graft copolymerization. [Monomer]:[initiator]:[catalyst]:[reducing agent]:[ligand] ratio was 428:1:32:320:48 for PVDF-*g*-PSPMAP copolymerization. After the 16 days reaction time the reaction flask was cooled and PVDF-*g*-PSPMAP graft copolymer was precipitated in excess water, filtered and dried in a vacuum oven at 50 °C. PVDF-*g*-PSPMAP graft copolymer was further purified by stirring for 24 h in an excess amount of THF at room temperature to remove the residual PSPMAP homopolymer if any. Purified PVDF-*g*-PSPMAP graft copolymer was filtered and dried in a vacuum oven at 50 °C. The THF non-soluble part of PVDF-*g*-PSPMAP graft copolymer was stirred for 5h at 100°C in boiling water to determine the solubility ratio of PVDF-*g*-PSPMAP graft copolymer.

#### **3.3.2 Synthesis of PVDF-*g*-PGMA Graft Copolymer**

AGET-ATRP procedure was performed as follows: catalyst, CuCl<sub>2</sub> (0.08 g, 6 x 10<sup>-4</sup> mol) and as reducing agent ascorbic acid (1.04 g, 6 x 10<sup>-3</sup> mol), was placed in a 100 ml of flask, which contained a side arm with a Teflon valve sealed with a Teflon stopper. Then the flask was deoxygenated three times by vacuum-nitrogen cycles, macroinitiator PVDF-107 (2 g, 1.87 x 10<sup>-5</sup> mol) priority dissolved in 40 ml of NMP at

80 °C, GMA (2 g,  $1.4 \times 10^{-2}$  mol) were added to flask, respectively, and the mixture was nitrogen bubbled for 30 min. Finally, ligand Me<sub>6</sub>-TREN (0.21 g,  $9 \times 10^{-4}$  mol) was added, then all liquid components were nitrogen bubbled again for 5 min. before the flask was replaced in thermostatically controlled oil bath at 100°C at 400 rpm stirring rate to initiate the graft copolymerization. [Monomer]:[initiator]:[catalyst]:[reducing agent]:[ligand] ratio was 749:1:32:320:48 for PVDF-*g*-PGMA copolymerization. After the 16 days reaction time the reaction flask was cooled and PVDF-*g*-PGMA graft copolymer was precipitated in excess water, filtered and dried in a vacuum oven at 50 °C. PVDF-*g*-PGMA graft copolymer was further purified by stirring for 24 h in an excess amount of THF at room temperature to remove the residual PGMA homopolymer if any. Purified PVDF-*g*-PGMA graft copolymer was filtered and dried in a vacuum oven at 50 °C.

### 3.3.3 Synthesis of PVDF-*g*-PEGMAP Graft Copolymer

AGET-ATRP procedure was performed as follows: catalyst, CuCl<sub>2</sub> (0.122 g,  $9 \times 10^{-4}$  mol) and as reducing agent ascorbic acid (1.56 g,  $9 \times 10^{-3}$  mol), was placed in a 100 ml of flask, which contained a side arm with a Teflon valve sealed with a Teflon stopper. Then the flask was deoxygenated three times by vacuum-nitrogen cycles, macroinitiator PVDF-107 (3 g,  $2.8 \times 10^{-5}$  mol) priory dissolved in 60 ml of NMP at 80 °C, EGMAP (2 g,  $1.4 \times 10^{-2}$  mol) were added to flask, respectively, and the mixture was nitrogen bubbled. Finally, ligand Me<sub>6</sub>-TREN (0.31 g,  $1.4 \times 10^{-3}$  mol) was added, then all liquid components were nitrogen bubbled again for 5 min. before the flask was replaced in thermostatically controlled oil bath at 100 °C at 400 rpm stirring rate to initiate the graft copolymerization. [Monomer]:[initiator]:[catalyst]:[reducing agent]:[ligand] ratio was 500:1:32:320:50 for PVDF-*g*-PEGMAP copolymerization. After the 15 days reaction time the reaction flask was cooled and PVDF-*g*-PEGMAP graft copolymer was precipitated in excess water, filtered and dried in a vacuum oven at 50 °C. PVDF-*g*-PEGMAP graft copolymer was further purified by stirring for 24 h in an excess amount of THF at room temperature to remove the residual PEGMAP homopolymer if any. Purified PVDF-*g*-PEGMAP graft copolymer was filtered and dried in a vacuum oven at 50 °C. PVDF-*g*-PEGMAP copolymer was stirred for 5h at 100 °C in boiling water to determine the solubility ratio of PVDF-*g*-PEGMAP graft copolymer.

### 3.3.4 Synthesis of PVDF-*g*-PHEA Graft Copolymer

AGET-ATRP procedure was performed as follows. Catalyst, CuCl<sub>2</sub> (0.08 g,  $6 \times 10^{-4}$  mol) and as reducing agent ascorbic acid (1.04 g,  $6 \times 10^{-3}$  mol), was placed in a 100 ml of flask, which contained a side arm with a Teflon valve sealed with a Teflon stopper. Then the flask was deoxygenated three times by vacuum-nitrogen cycles, macroinitiator PVDF-107 (2 g,  $1.87 \times 10^{-5}$  mol) priority dissolved in 40 ml of NMP at 80 °C, HEA (2 g,  $1.7 \times 10^{-2}$  mol) were added to flask, respectively, and the mixture was nitrogen bubbled for 30 min.. Finally, ligand Me<sub>6</sub>-TREN (0.21 g,  $9 \times 10^{-4}$  mol) was added, and then all liquid components were nitrogen bubbled for 5 min. before the flask was replaced in thermostatically controlled oil bath at 100 °C at 400 rpm stirring rate to initiate the graft copolymerization. [Monomer]:[initiator]:[catalyst]:[reducing agent]:[ligand] ratio was 921:1:32:320:48 for PVDF-*g*-PHEA copolymerization. After the 31 days reaction time the reaction flask was cooled and PVDF-*g*-PHEA graft copolymer was precipitated in excess water. Then PVDF-*g*-PHEA graft copolymer was filtered and dried in a vacuum oven at 50 °C.

PVDF-*g*-PHEA graft copolymer was further purified by stirring for 24 h in an excess amount of THF at room temperature to remove the residual PHEA homopolymer if any. Purified PVDF-*g*-PHEA graft copolymer was filtered and dried in a vacuum oven at 50 °C.

### 3.3.5 Synthesis of PVDF-*g*-PHEMA Graft Copolymer

AGET-ATRP procedure was performed as follows: catalyst, CuCl<sub>2</sub> (0.08 g,  $6 \times 10^{-4}$  mol) and as reducing agent ascorbic acid (1.04 g,  $6 \times 10^{-3}$  mol), was placed in a 100 ml of flask, which contained a side Teflon valve sealed with a Teflon stopper. Then the flask was deoxygenated three times by vacuum-nitrogen cycles, macroinitiator PVDF-107 (2 g,  $1.87 \times 10^{-5}$  mol) priority dissolved in 40 ml of DMF at 80 °C, and HEMA (2 g,  $1.5 \times 10^{-2}$  mol) were added to flask, respectively, and the mixture was nitrogen bubbled for 30 min. Finally ligand Me<sub>6</sub>-TREN (0.21 g,  $9 \times 10^{-4}$  mol) was added, then all liquid components were nitrogen bubbled again for 5 min. before the flask was replaced in thermostatically controlled oil bath at 100 °C at 400 rpm stirring rate to initiate the graft copolymerization.

[Monomer]:[initiator]:[catalyst]:[reducing agent]:[ligand] ratio was 822:1:32:320:48 for PVDF-*g*-PHEMA copolymerization. After the 31 days reaction time the reaction flask was cooled and PVDF-*g*-PHEMA graft copolymer was precipitated in excess water. Then PVDF-*g*-PHEMA graft copolymer was filtered and dried in a vacuum oven at 50 °C.

PVDF-*g*-PHEMA graft copolymer was further purified by stirring for 24 h in an excess amount of THF at room temperature to remove the residual PHEMA homopolymer if any. Purified PVDF-*g*-PHEMA graft copolymer was filtered and dried in a vacuum oven at 50 °C. PVDF-*g*-PHEMA copolymer was stirred for 5h at 100°C in boiling water to determine the solubility ratio of PVDF-*g*-PHEMA graft copolymer.

### **3.3.6 Synthesis of PVDF-*g*-PAMPS Graft Copolymer**

AGET-ATRP procedure was performed as follows. Catalyst, CuCl<sub>2</sub> (0.08 g, 6 x 10<sup>-4</sup> mol) and as reducing agent ascorbic acid (1.04 g, 6 x 10<sup>-3</sup> mol), was placed in a 100 ml of flask, which contained a side Teflon valve sealed with a Teflon stopper. Then the flask was deoxygenated three times by vacuum-nitrogen cycles, macroinitiator PVDF-107 (2 g, 1.87 x 10<sup>-5</sup> mol) priority dissolved in 40 ml of NMP at 80 °C, AMPS (2 g, 1 x 10<sup>-2</sup> mol) were added to flask, respectively, and the mixture was nitrogen bubbled for 30 min.. Finally, ligand Me<sub>6</sub>-TREN (0.21 g, 9 x 10<sup>-4</sup> mol) was added, then all liquid components were nitrogen bubbled again for 5 min. before the flask was replaced in thermostatically controlled oil bath at 100 °C at 400 rpm stirring rate to initiate the graft copolymerization. [Monomer]:[initiator]:[catalyst]:[reducing agent].[ligand] ratio was 534:1:32:320:48 for PVDF-*g*-PAMPS copolymerization. After the 31 days reaction time the reaction flask was cooled and PVDF-*g*-PAMPS graft copolymer was precipitated in excess water. PVDF-*g*-PAMPS graft copolymer was filtered and dried in a vacuum oven at 50 °C.

PVDF-*g*-PAMPS graft copolymer was further purified by stirring for 24 h in an excess amount of THF at room temperature to remove the residual PAMPS homopolymer if any. Purified PVDF-*g*-PAMPS graft copolymer was filtered and dried in a vacuum oven at 50 °C. PVDF-*g*-PAMPS copolymer was stirred for 5h at

100 °C in boiling water to determine the solubility ratio of PVDF-*g*-PAMPS graft copolymer

### 3.3.7 Synthesis of PVDF-*g*-PVPA Graft Copolymer

AGET-ATRP procedure was performed as follows: catalyst, CuCl<sub>2</sub> (0.08 g, 6 x 10<sup>-4</sup> mol) and as reducing agent ascorbic acid (1.04 g, 6 x 10<sup>-3</sup> mol), was placed in a 100 ml of flask, which contained a side arm with a Teflon valve sealed with a Teflon stopper. Then the flask was deoxygenated three times by vacuum-nitrogen cycles, macroinitiator PVDF-107 (2 g, 1.87 x 10<sup>-5</sup> mol) priority dissolved in 40 ml of DMF at 80 °C, VPA (2 g, 1.85 x 10<sup>-2</sup> mol) were added to the flask, respectively, and the mixture was nitrogen bubbled for 30 min. Finally, ligand Me<sub>6</sub>-TREN (0.21 g, 9 x 10<sup>-4</sup> mol) was added, then all liquid components were nitrogen bubbled again for 5 min. before the flask was replaced in thermostatically controlled oil bath at 100°C at 400 rpm stirring rate to initiate the graft copolymerization. [Monomer]:[initiator]:[catalyst]:[reducing agent]:[ligand] ratio was 990:1:32:320:48 for PVDF-*g*-PVPA copolymerization. After the 19 days reaction time the reaction flask was cooled and PVDF-*g*-PVPA graft copolymer was precipitated in excess water. Finally PVDF-*g*-PVPA graft copolymer was filtered and dried in a vacuum oven at 50 °C.

PVDF-*g*-PVPA graft copolymer was further purified by stirring for 24 h in an excess amount of THF at room temperature to remove the residual PVPA homopolymer if any. Purified PVDF-*g*-PVPA graft copolymer was filtered and dried in a vacuum oven at 50 °C. Then PVDF-*g*-PVPA copolymer was stirred for 5h at 100 °C in boiling water to determine the solubility ratio of PVDF-*g*-PVPA graft copolymer

### 3.4 Characterization

Molecular weight and molecular weight distributions of polymers were measured by using a gel permeation chromatography (GPC) system consisting of an Agilent 1200 series pump, a Waters Styragel HR column (2) and BI-MwA light scattering detector, with a DMF flow rate 0.5 ml.min<sup>-1</sup>.

FT-IR reflectance spectrums of polymers were recorded on a Bruker Equinox 55 Spectrum One FT-IR spectrometer with a Universal ATR attachment with diamond

and ZnSe tip.

The  $^1\text{H}$ -NMR spectrum was recorded on a Varian AS 500 NMR Spectrometer (500 MHz) in  $\text{CDCl}_3$  and  $d\text{-DMF}$  using tetramethylsilane (TMS) as an internal standard.

The thermal properties of the PVDF based graft copolymers samples were measured by TGA and DSC analyses. The polymer samples were heated to  $600\text{ }^\circ\text{C}$  at a heating rate of  $50\text{ }^\circ\text{C min}^{-1}$  under a dry nitrogen atmosphere by Netzsch STA 449C TGA.

DSC characterization was made by heating and cooling the graft copolymer samples between  $-159\text{ }^\circ\text{C}$  and  $350\text{ }^\circ\text{C}$  at a heating rate of  $20\text{ }^\circ\text{C min}^{-1}$  under a dry nitrogen atmosphere.

## 4. RESULTS and DISCUSSION

### 4.1 Synthesis of PVDF-Based Graft Copolymers by ATRP

Immobilization of hydrophilic monomers onto the hydrophobic PVDF backbone graft copolymerisation was achieved via ATRP as described in experimental part. The copolymerization conditions and results are given in Table 4.1. Only graft copolymers of PVDF with PAA (PVDF-*g*-PAA), PSPMAP (PVDF-*g*-PSPMAP), PSAPMA-TEA (PVDF-*g*-PSAPMA-TEA), PHEMA (PVDF-*g*-PHEMA), PS (PVDF-*g*-PS) graft copolymers were able to synthesize by ATRP whereas PVPA (PVDF-*g*-PVPA), PAMPS (PVDF-*g*-PAMPS), PHEA (PVDF-*g*-PHEA) and PGMA (PVDF-*g*-PGMA) graft copolymers were not obtained. PGMA, PVPA, PAMPS and PHEA that might not co-operated with hydrophobic PVDF-107 macroinitiator. Acrylic monomer acidic group containing AMPS, VPA and also hydroxyl group containing HEA gave polymer gels during the ATRP polymerization method. [46]

**Table 4.1:** Reaction Conditions and Results of PVDF-Based Graft Copolymers

Run (#)	Macroinitiator (PVDF-107K, 10 <sup>-5</sup> mol)	Monomer (10 <sup>-2</sup> mol)	Temp. (°C)	Time (day)	THF-ns <sup>f</sup> (%)	Conv. <sup>g</sup> (%)
NB-1 <sup>a</sup>	1.6	<i>t</i> BA (17)	90	1	36	47
NB-2 <sup>b</sup>	4.67	SPMAP (1.02)	100	22	100	84
NB-3 <sup>c</sup>	0.234	SAPMA-TEA (0.51)	100	18	100	66.4
NB-4 <sup>d</sup>	1.87	HEMA (3.12)	80	3	95	5
NB-5 <sup>e</sup>	4.67	S (17.5)	100	14	52.3	56.2

<sup>a</sup> PVDF-*g*-*t*BA, [M]<sub>0</sub>: [I]<sub>0</sub>: [CuCl]<sub>0</sub>: [PMDETA]<sub>0</sub> = 835:1:21:26 in DMF.

<sup>b</sup> PVDF-*g*-PSPMA, [M]<sub>0</sub>: [I]<sub>0</sub>: [CuCl]<sub>0</sub>: [PMDETA]<sub>0</sub> = 2184:1:21:26 in DMF.

<sup>c</sup> PVDF-*g*-PSAPMA-TEA, [M]<sub>0</sub>: [I]<sub>0</sub>: [CuCl]<sub>0</sub>: [PMDETA]<sub>0</sub> = 2179:1:43:51 in DMF.

<sup>d</sup> PVDF-*g*-PHEM, [M]<sub>0</sub>: [I]<sub>0</sub>: [CuCl]<sub>0</sub>: [PMDETA]<sub>0</sub> = 1670:1:83:83 in DMF.

<sup>e</sup> PVDF-*g*-PS, [M]<sub>0</sub>: [I]<sub>0</sub>: [CuCl]<sub>0</sub>: [Me<sub>6</sub>-TREN]<sub>0</sub> = 4255:1:8:25 in NMP.

<sup>f</sup> The insoluble part of *t* graft copolymer after purification process by TFA.

<sup>g</sup> Conversions were calculated by gravimetric measurements.

Thermal stability is of crucial importance for membrane materials. Table 4.2 presents the thermal decomposition temperatures of synthesised PVDF-based graft copolymers compared to Nafion-117 and PVDF-107.

**Table 4.2:** Thermal Decomposition Temperatures of PVDF-Based Graft Copolymers

Run (#)	5% Decomp. Temp. (°C)	10 %Decomp. Temp. (°C)	20% Decomp. Temp. (°C)
Nafion-117	305.4	357.5	440.6
PVDF-107	447.1	462.1	473.1
NB-1 <sup>a</sup>	154.9	175.6	254.8
NB-2 <sup>b</sup>	395.9	409.0	424.2
NB-3 <sup>c</sup>	282.0	309.0	346.3
NB-4 <sup>d</sup>	380.6	411.3	435.3

<sup>a</sup> PVDF-*g*-*Pt*BA graft copolymer

<sup>b</sup> PVDF-*g*-PSPMAP graft copolymer

<sup>c</sup> PVDF-*g*-PSAPMA-TEA graft copolymer

<sup>d</sup> PVDF-*g*-PHEMA graft copolymer

<sup>e</sup> PVDF-*g*-PS graft copolymer

The synthesized PVDF-based copolymer should be consists of hydrophilic and hydrophobic domains. Hydrophilic regions allow transport of protons from anode to cathode in fuel cell assembly the hydrophobic region offers good mechanical strength. The PVDF-*g*-*Pt*BA, was modified to include hydrophilic ionic moieties obtained by hydrolysis with TFA at room temperature. The hydrolysis of *Pt*BA grafts resulted in amphiphilic graft copolymers with hydrophilic PAA side chains. The steps of PVDF-*g*-PAA graft copolymers synthesis are shown as representatively Figure 4.1 and 4.2.

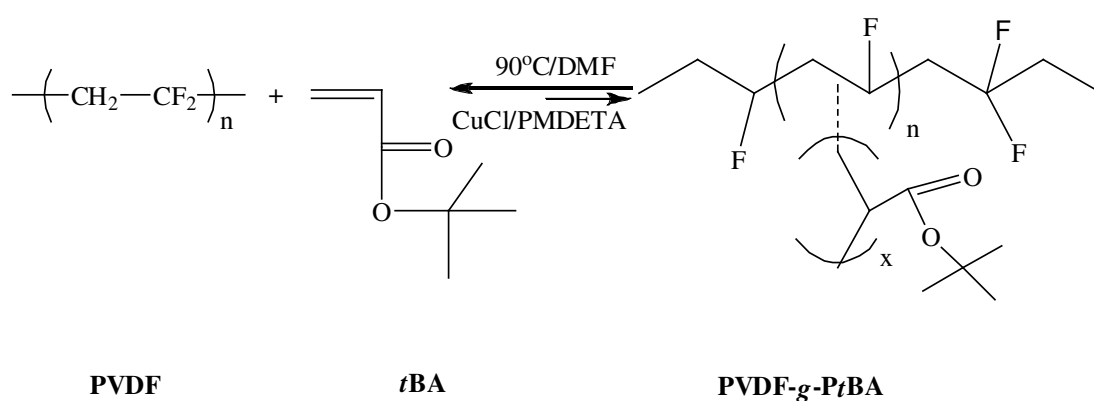


**Figure 4.1:** Synthesis of PVDF-*g*-*Pt*BA Graft Copolymer

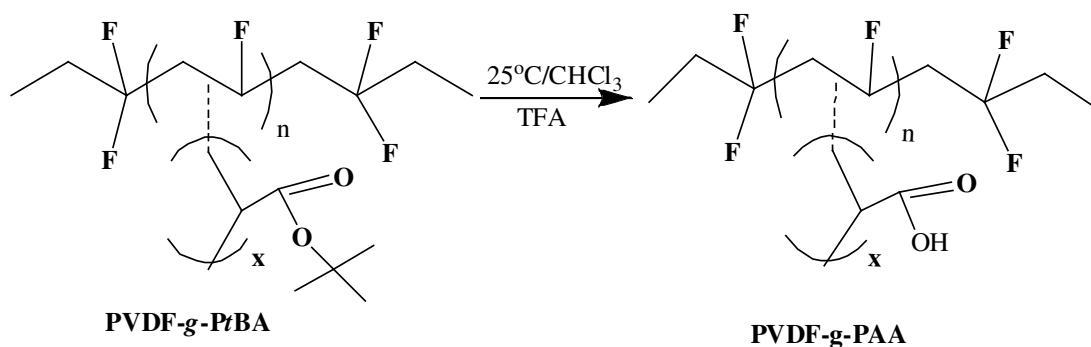


**Figure 4.2:** Synthesis of PVDF-g-PAA Graft Copolymer

ATR FT-IR spectrum of PVDF-g-PAA graft copolymer is shown in Figure 4.3. In ATR FT-IR spectrum of PVDF-g-PAA, strong carbonyl ( $\text{-C=O}$ ) group stretching vibration band at  $1702\text{ cm}^{-1}$  and at about  $3400\text{ cm}^{-1}$  hydroxyl ( $\text{-OH}$ ) group band and the characteristic peaks of PVDF between  $1450\text{-}668\text{ cm}^{-1}$  explain that the PVDF-g-PAA graft copolymerization was achieved.

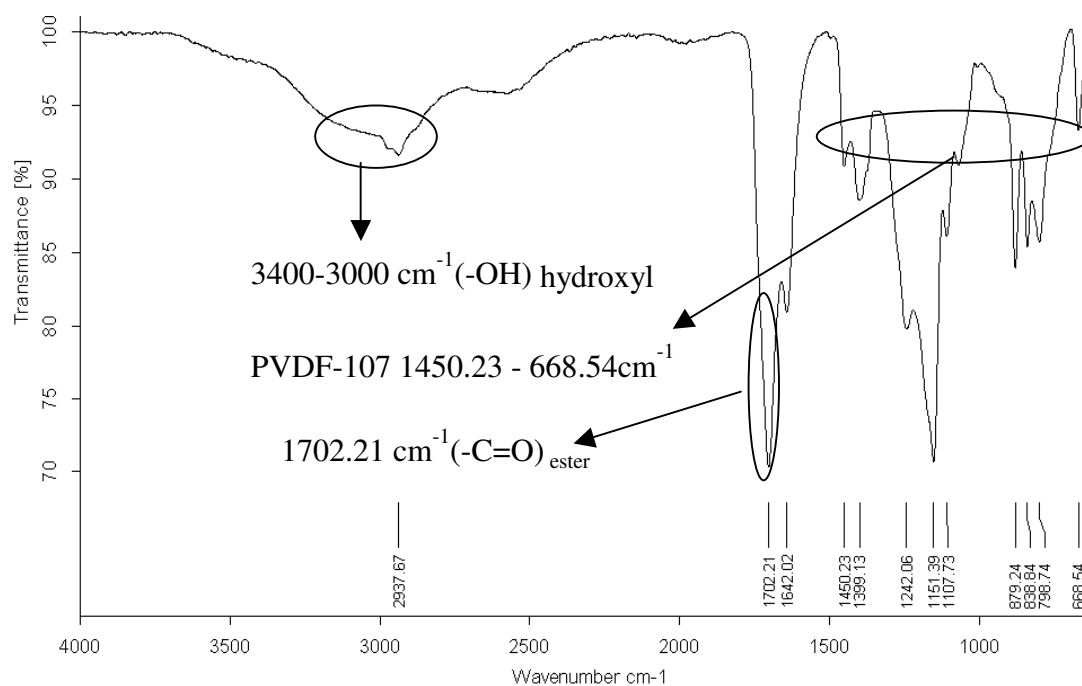


**Figure 4.3:** ATR FT-IR Spectrum of PVDF-g-PAA Graft Copolymer

The thermal stability of PVDF-107, Nafion-117 and PVDF-g-PAA graft copolymers is studied by TGA analysis. Figure 4.4 shows the respective TGA curves of PVDF-107 homopolymer and Nafion-117 graft copolymer. The decomposition of PVDF-107 homopolymer starts at about 450 °C due to the -CF<sub>2</sub>- group on the PVDF backbone. The shielding effect of the fluorine atoms adjacent to the -CH<sub>2</sub> groups provides to the polymer a good thermal stability. PVDF-117 shows a  $T_g$  at -40.8 °C and  $T_m$  at 171.5 °C on the DSC graphic.

On the TGA graphic of Nafion-117, three distinct peaks are shown. The weight loss curve of Nafion-117 shows a weight loss of about 5 % at 305.4 °C. Another 10 % of the weight lost at 357.5 °C. Above 400 °C, the final decomposition of Nafion-117 begins, losing all mass by 600 °C.

The initial peak between 75 °C and 300 °C can be attributed to the loss of residual water in the Nafion-117. The second peak between 300 °C and 400 °C is due to the decomposition of sulphonic acid groups in the Nafion-117 sample. [47]

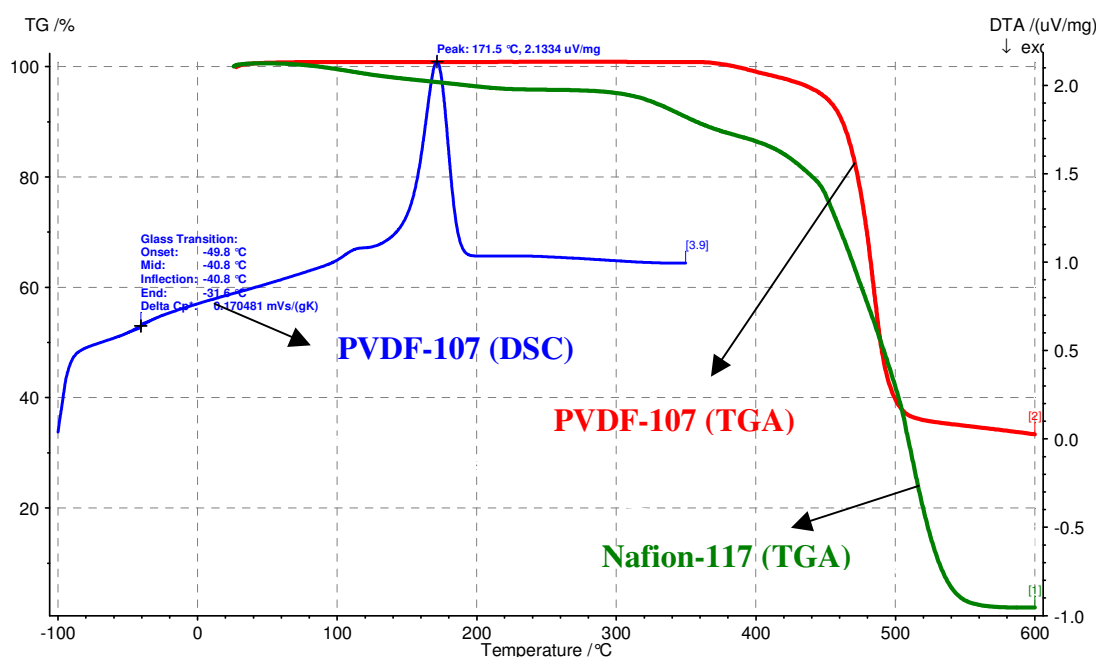


**Figure 4.4:** TGA and DSC Graphics of PVDF-107 and Nafion-117

Figure 4.5 the TGA curves of PVDF homopolymer and PVDF-g-PAA graft copolymer were compared. A distinct three-step degradation process is observed for the PVDF-g-PAA graft copolymer sample. The onset of the first major weight loss at about 100 °C corresponds to the loss of residual water. The second major weight loss begins at about 200 °C, corresponding to the decomposition of the AA polymer. The

last major weight loss begins at about 400 °C, corresponding to the decomposition of the PVDF main chain. At about 150 °C, 300 °C, and 400 °C, 5 %, 30 %, and 50 % weight loss were observed, respectively.

However, compared to PVDF, the thermal stability of PVDF-*g*-PAA graft copolymer was observed to be inferior. [48] According to the Figure 4.4, the PVDF-*g*-PAA graft copolymer is inappropriate for fuel cell membrane applications because of its decomposition starts at fuel cell working temperature, additionally weight loss of over 50 %, compared to Nafion-117, at over 400 °C.

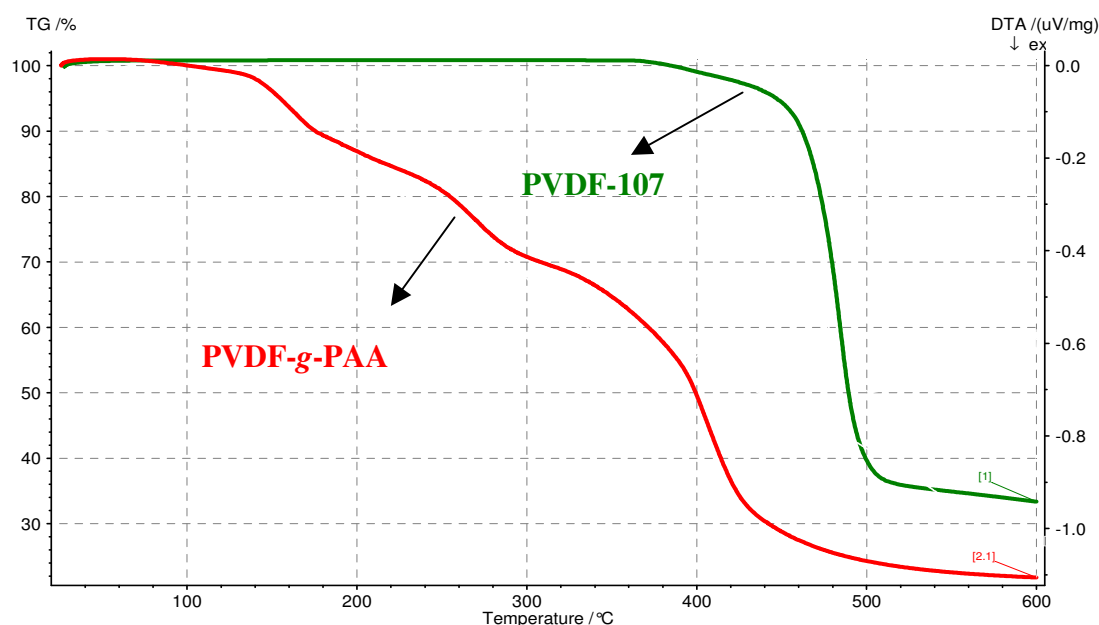


**Figure 4.5:** TGA Graphics of PVDF-107 and PVDF-*g*-PAA Graft Copolymer

Generally the fluoro polymers, which are used in fuel cells, should present thermal stability as well as hydrolytic stability for fuel cell membrane operating conditions. [49] The solubility ratio of PVDF-*g*-PAA was 40 % in water at 100 °C that also classifies it as inappropriate for fuel cell membrane in the operating conditions.

Due to the insolubility of SPMAP monomer in DMF, the synthesis of the PVDF-*g*-PSPMAP graft copolymer was carried out in heterogeneous condition (Figure 4.6).



The solubility ratio of the PVDF-*g*-PSPMAP graft copolymer was 71 % at 100 °C in water. PVDF homopolymer is hydrophobic in nature; therefore, that clearly indicates that the grafting of SPMAP monomers improved the solubility of PVDF in water.

The resulted graft copolymer PVDF-*g*-PSPMAP could not find any potential applications such as membranes for fuel cells due to its high solubility ratio in water and insolubility in organic solvents.

SPMAP was modified to SAPMA monomer by hydrolysis with TFA at room temperature in order to solubilize in DMF (Figure 4.8). However acidic monomers have not yet been successfully polymerised by ATRP, because they can protonate ligands and form the corresponding carboxylate salts. [13]

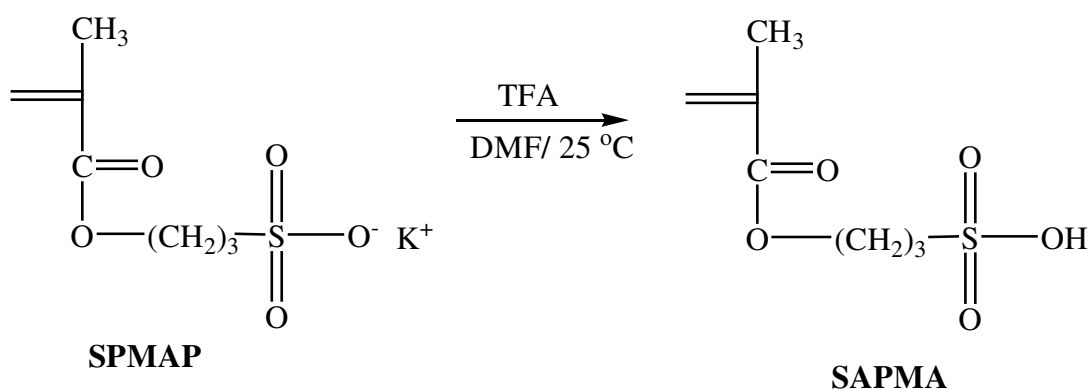


**Figure 4.8:** Synthesis of SAPMA Monomer

Hence, SAPMA monomer was converted to the SAPMA-TEA monomer (DMF soluble) by triethylamine (Figure 4.9).

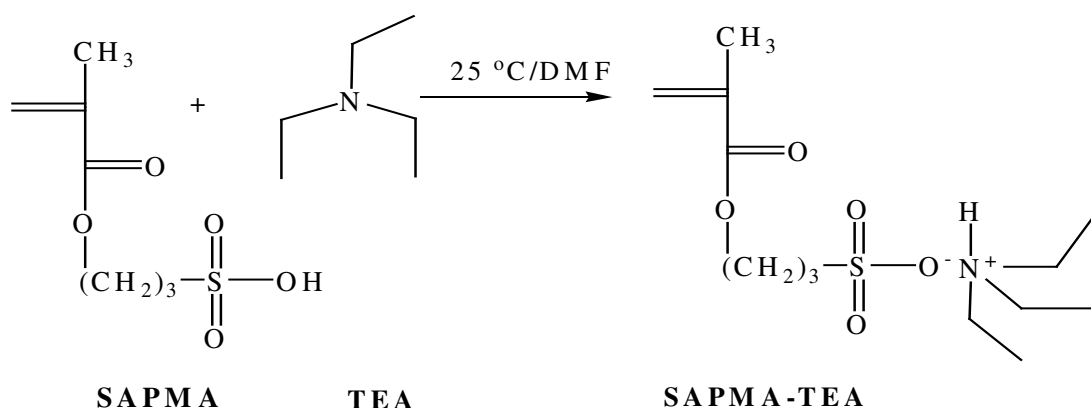


**Figure 4.9:** Synthesis of SAPMA-TEA Monomer

The steps of PVDF-*g*-PSAPMA-TEA graft copolymer synthesis are shown in Figure 4.10. Due to the insolubility in DMF, THF, DMSO, CHCl<sub>3</sub> solvents PVDF-*g*-

PSAPMA-TEA graft copolymer could not characterised by GPC (DMF) and  $^1\text{H}$  NMR (d-DMF).

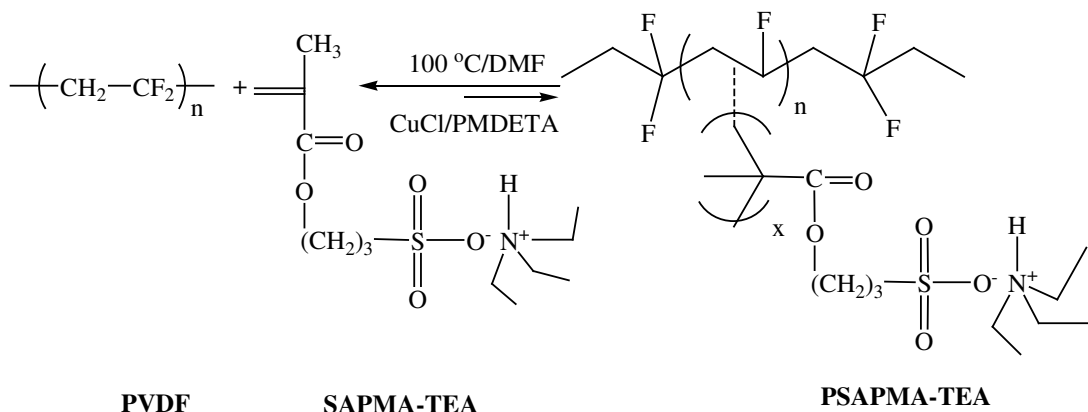


**Figure 4.10:** Synthesis of PVDF-*g*-PSAPMA-TEA Graft Copolymer

The thermal stability of the PVDF-*g*-PSAPMA-TEA graft copolymers is studied by TGA and DSC analysis (Figure 4.11). TEA and the sulphonic acid group decomposition begin at 260.9 °C. The decomposition at this temperature continues with steeping slope and comes to the end at 600 °C with a total weight loss of 60 %. Compared to PVDF-*g*-PAA and Nafion-117, PVDF-107, PVDF-*g*-PSAPMA-TEA graft copolymer is dramatically more thermally stable.

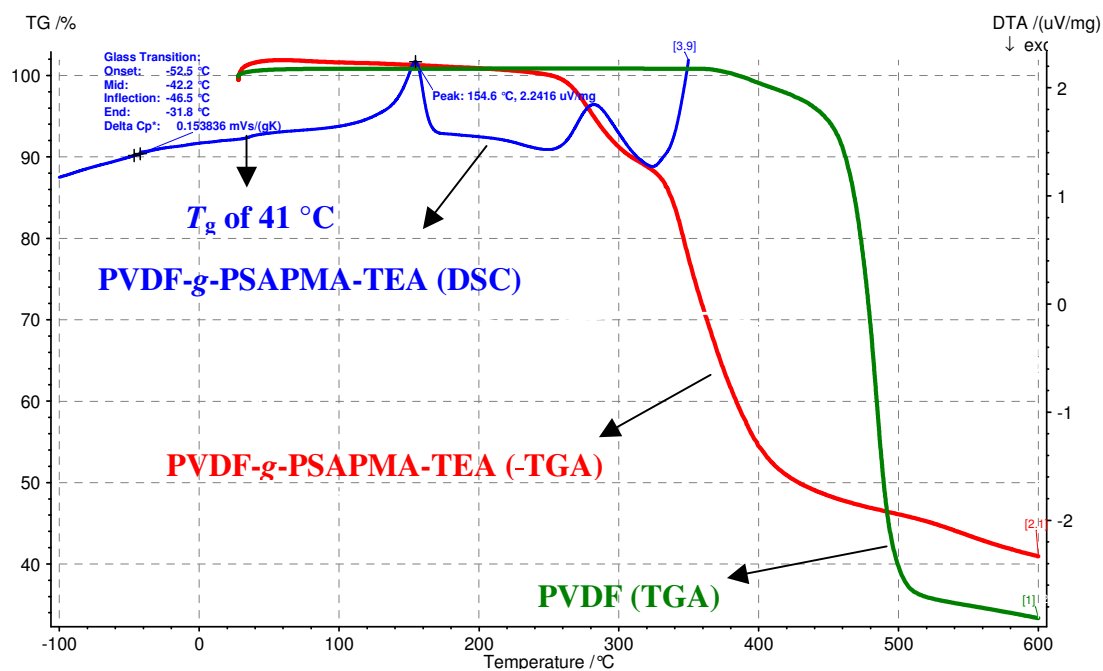


**Figure 4.11:** TGA and DSC Graphics of PVDF-107 and PVDF-*g*-PSAPMA-TEA Graft Copolymer

Despite the high thermal stability of PVDF-*g*-PSAPMA-TEA graft copolymer, its solubility ratio was 74 % at 100 °C in water. Compared to PVDF-*g*-PAA graft copolymer their solubility is nearly same, therefore it could not applied as membranes for fuel cells. While DSC graphic of the PVDF-117 shows a  $T_g$  at -40.8 °C and  $T_m$  at 171.5 °C in Figure 4.4, PVDF-*g*-PSAPMA-TEA graft copolymer shows  $T_g$  at -42.2 and 41 °C and  $T_m$  at 154.6 °C (Figure 4.11). Thus, the grafting of SAPMA-TEA onto PVDF chain was observed.

To synthesize ATRP precursor, which possesses ionic moieties, HEMA with -OH functional group was grafted on to the PVDF backbone via ATRP. The steps of PVDF-*g*-PHEMA graft copolymer synthesis are presented in Figure 4.12.

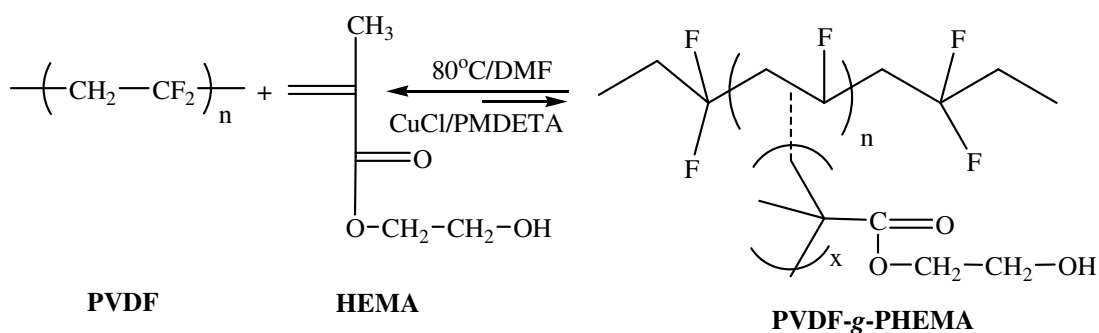


**Figure 4.12:** Synthesis of PVDF-*g*-PHEMA Graft Copolymer

As representatively, ATR FT-IR spectrum of PVDF-*g*-PHEMA graft copolymer is shown in Figure 4.13. In ATR FT-IR spectrum of PVDF-*g*-PHEMA, carbonyl group (-C=O) stretching vibration band at 1717.61  $\text{cm}^{-1}$ , at about 3400  $\text{cm}^{-1}$  hydroxyl group (-OH) band and the characteristic bands of PVDF between 1400-740  $\text{cm}^{-1}$  explain that the PVDF-*g*-PHEMA graft copolymerization was achieved.

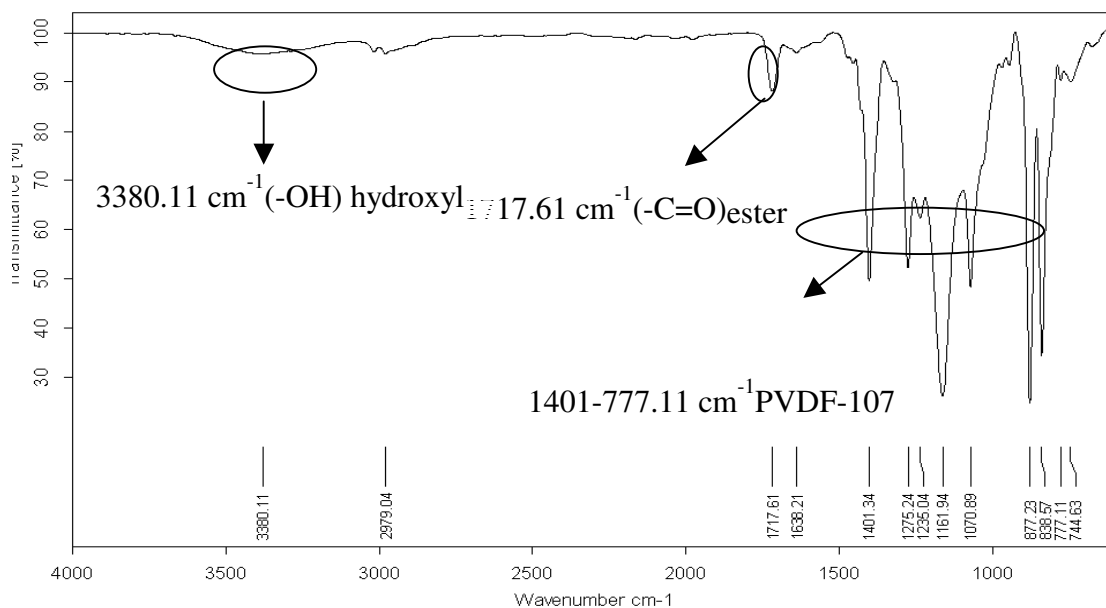


**Figure 4.13:** ATR FT-IR Spectrum of PVDF-*g*-PHEMA Graft Copolymer

The thermal stability of the PVDF-*g*-PHEMA graft copolymer is studied by TGA and DSC analyses (Figure 4.14). It is well known that degradation range of the functional groups in polymethacrylates is 240 °C–280 °C and total decomposition of the monomer units starts above 310 °C. [50] Due to the high stability of the PVDF-*g*-PHEMA graft copolymer decomposition begins at 310 °C with onset 419.8 °C and decomposition will continue till 480 °C. This observation and obtained shift of decomposition curve for the sample compare to PVDF is taken account of graft copolymerisation. Compared to PVDF-*g*-PAA graft copolymer and PVDF-*g*-PSAPMA-TEA graft copolymer, PVDF-*g*-PHEMA graft copolymer is distinctively more thermally stable. According to the Figure 4.14, PVDF-*g*-PHEMA graft copolymer shows  $T_g$  at  $-41.9$  and  $20$  °C and  $T_m$  at  $166.2$  °C while PVDF-107 shows a  $T_g$  at  $-40.8$  °C and  $T_m$  at  $171.5$  °C in Figure 4.4. The  $T_g$  and the  $T_m$  of the graft copolymer were compared to PVDF-107 as a result of the grafting.

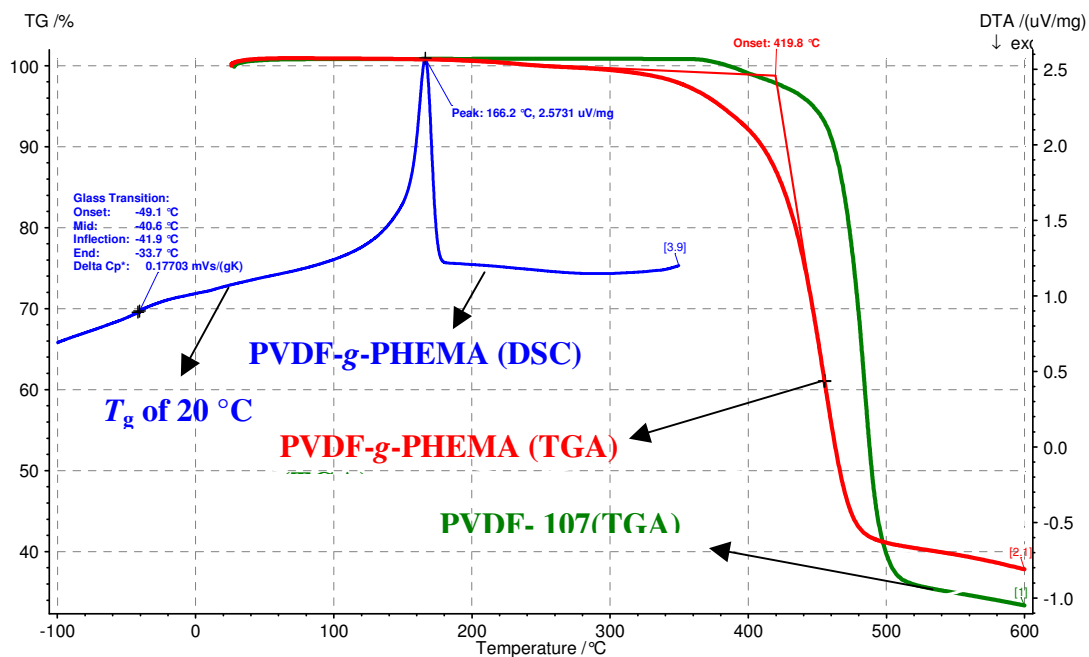


**Figure 4.14:** TGA and DSC Graphics of PVDF-107 and PVDF-g-PHEMA Graft Copolymer

<sup>1</sup>H NMR (d-DMF) spectrum of the PVDF-g-PHEMA provides further evidence of grafting HEMA (Figure 4.15).

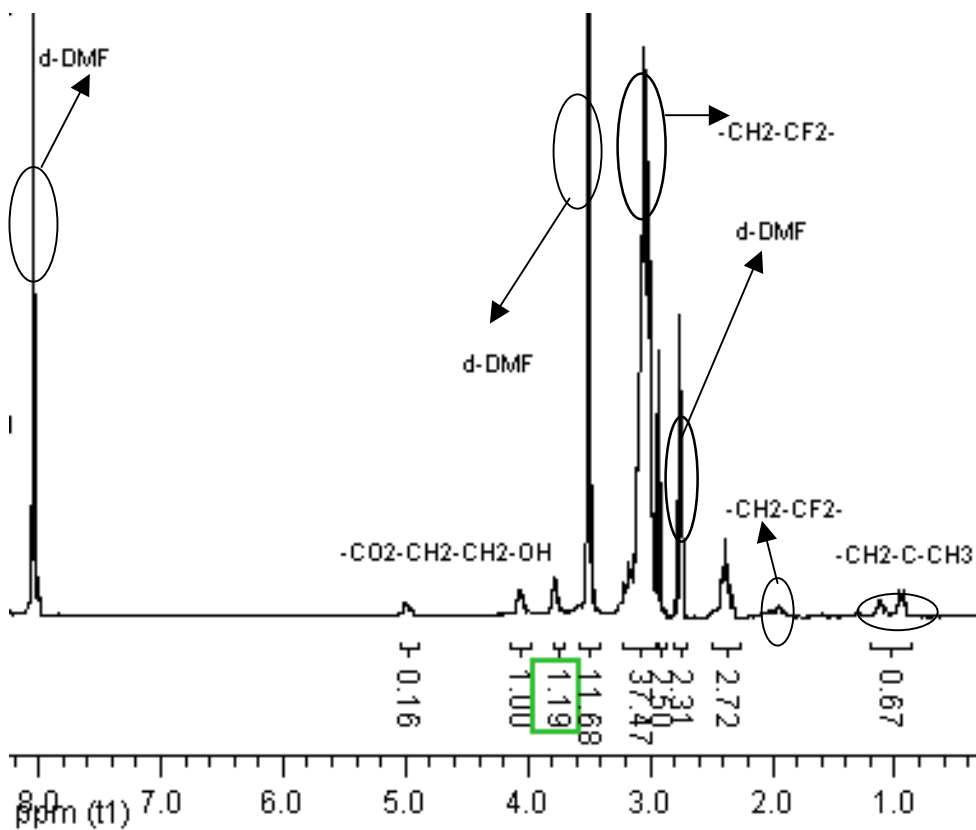


**Figure 4.15:** <sup>1</sup>H NMR (d-DMF) Spectrum of PVDF-g-PHEMA Graft Copolymer

The peaks of solvent d-DMF are appeared at 2.7 ppm, 2.9 ppm and 8.2 ppm. Two peaks of 2.4 ppm and 3 ppm are corresponding to the hydrogen for  $-\underline{\text{C}}\text{H}_2\text{-CF}_2\text{-}$ . The peaks in the region of 5 – 3.6 ppm are corresponding to the hydrogens for  $-\underline{\text{C}}\text{H}_2\text{-CF}_2$  and  $\underline{\text{C}}\text{H}_2\text{-CH}_2\text{-OH}$ . The peaks of 2 ppm and 1 ppm are corresponding to the hydrogens for  $-\underline{\text{C}}\text{H}_2\text{-C-CH}_3$ , respectively. 3 mol % PHEMA and 97 mol % PVDF was calculated from the m/n ratio using corresponding peaks both for HEMA and PVDF.

In order to obtain other alternative proton exchange membrane to Naffion-117, styrene monomers are also grafted to the PVDF-107 backbone via ATRP. The synthesis of PVDF-*g*-PS graft copolymer is shown as representatively in Figure 4.16. The resulted graft copolymer was functionalized with sulphonic acid groups by sulphonation process in Figure 4.21. Hydrophilic sulphonic acid groups could facilitate the transport of protons during the applications such as membranes for fuel cells.

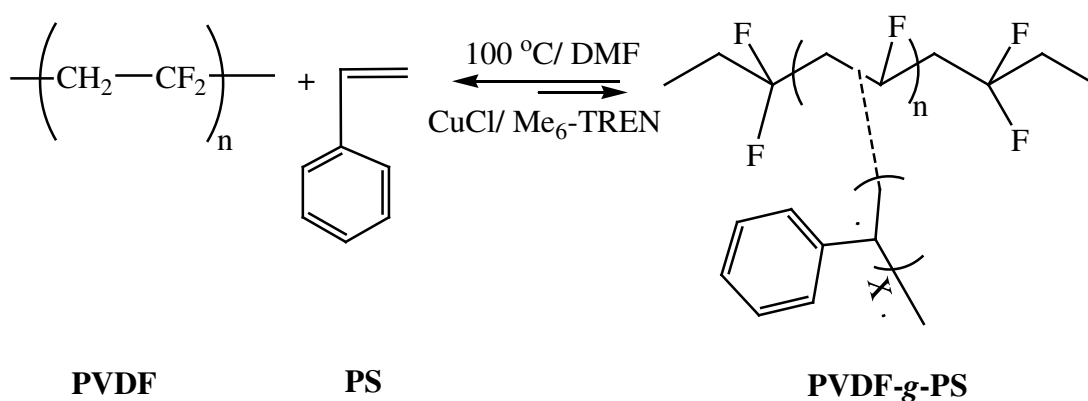


**Figure 4.16:** Synthesis of PVDF-*g*-PS Graft Copolymer

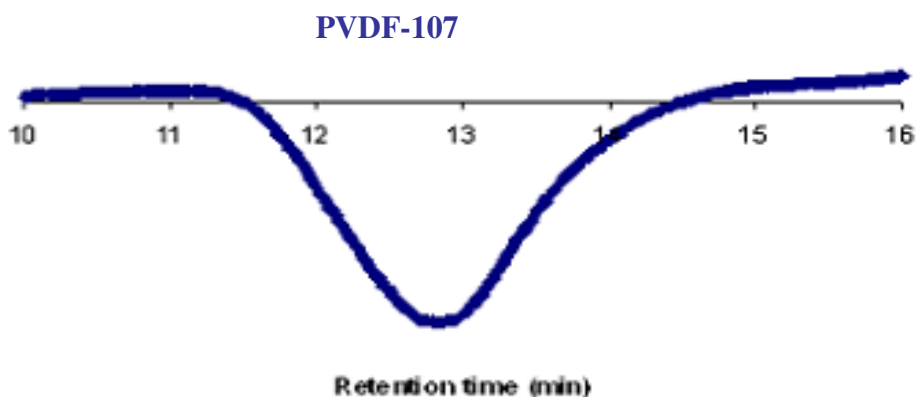


**Figure 4.17** GPC Graphic of PVDF-107 Macroinitiator

The representative GPC result is presented in Figure 4.18 provides further evidence of grafting S to PVDF backbone. As can be seen from the Figure 4.17, the initial negative refractive index signal (relative to DMF) of the PVDF-107 [9] changed to positive and shifted to the higher molecular weights by incorporation of S monomer (Figure 4.18).

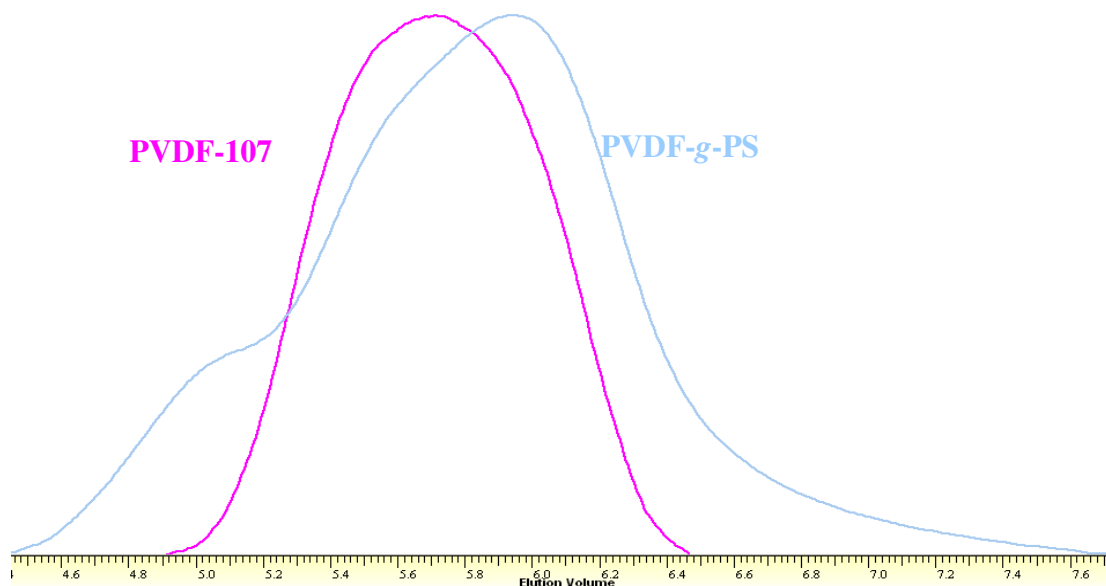


**Figure 4.18** GPC Traces of PVDF-107 (RI detector) and PVDF-g-PS (RI detector) Graft Copolymer

As representatively, ATR FT-IR spectrum of PVDF-g-PS graft copolymer is presented in Figure 4.19. In ATR FT-IR spectrum of PVDF-g-PS, aromatic proton stretching vibration band at  $1600\text{--}1400\text{ cm}^{-1}$ , aromatic proton stretching vibration

band at about  $3026\text{ cm}^{-1}$  and characteristic PVDF-107 bands at  $1467\text{-}695\text{ cm}^{-1}$  explain that the S monomers was grafted to the macroinitiator PVDF-107 homopolymer backbone.

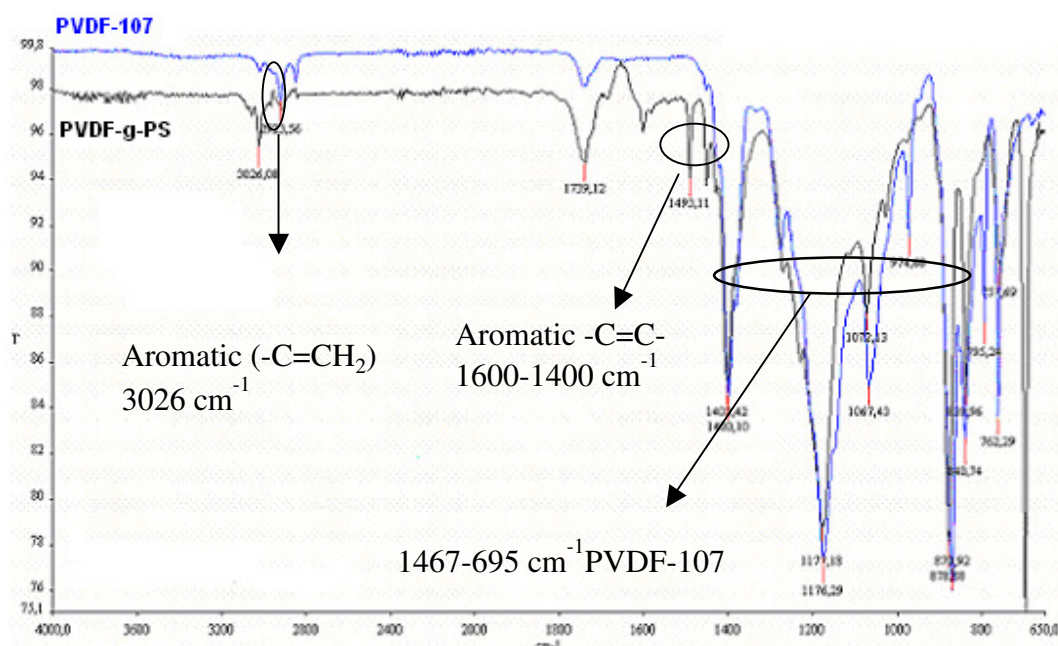


**Figure 4.19:** ATR FT-IR Spectrum of Macroinitiator PVDF-107 and PVDF-g-PS Graft Copolymer

As representatively,  $^1\text{H}$  NMR (d-DMF) Spectrum of PVDF-g-PS graft copolymer is presented in Figure 4.20. Grafting of PS to PVDF resulted in the appearance of peaks in the region of 7.2-6.4 ppm, corresponding to the aromatic hydrogen and the peaks in the region of 3.2 - 1.4 ppm are corresponding to the aliphatic hydrogen for PVDF and S. 13 mol % PS and 87 mol % PVDF was calculated from the m/n ratio using corresponding peaks both for S and PVDF.

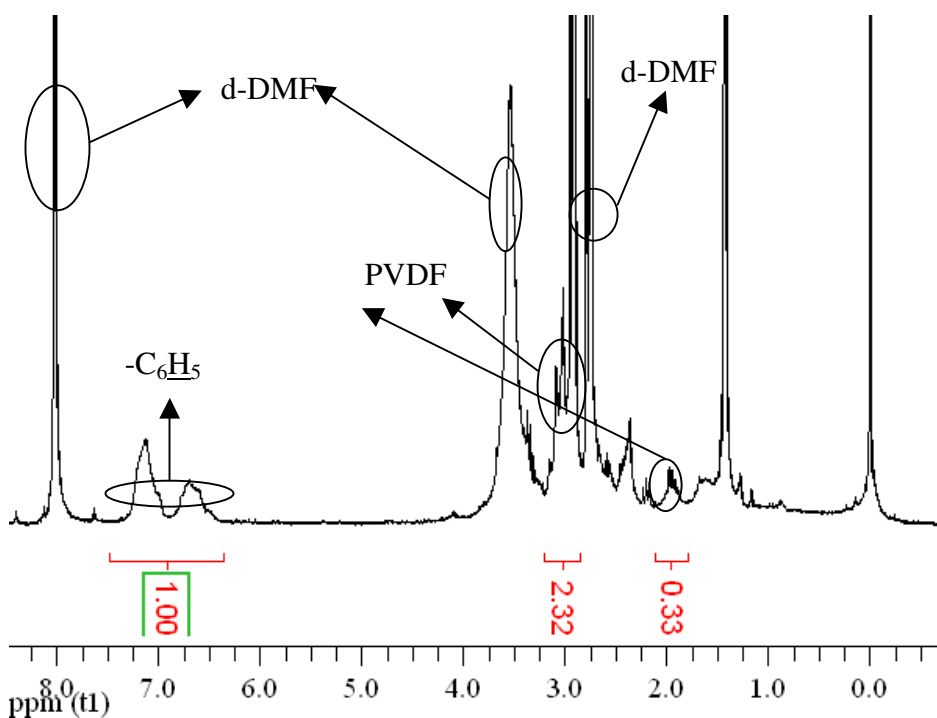


**Figure 4.20:**  $^1\text{H}$  NMR (d-DMF) Spectrum of PVDF-*g*-PS Graft Copolymer

The sulfonation process for PVDF-*g*-PS graft copolymer is presented in the Figure 4.21.

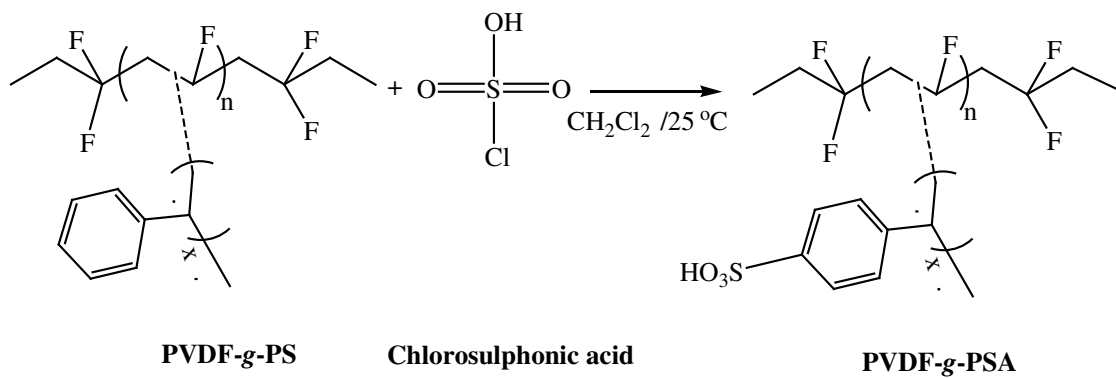


**Figure 4.21:** Synthesis of PVDF-*g*-PSA Graft Copolymer

The  $^1\text{H}$  NMR (d-DMF) spectrum of sulphonated PVDF-*g*-PSA is presented in the figure 4.22. Sulfonation of PS resulted in the appearance of peaks in the region 7.2-6.4 ppm, corresponding to the hydrogen for  $-\text{C}_6\text{H}_4-$  and the peaks in the region of 3.2 ppm - 1.4 ppm are corresponding to the hydrogen for  $-\text{CH}_2-\text{CF}_2$ . 87 mol % PSA and 13 mol % PS was calculated from the m/n ratio using corresponding peaks both for S and SA.

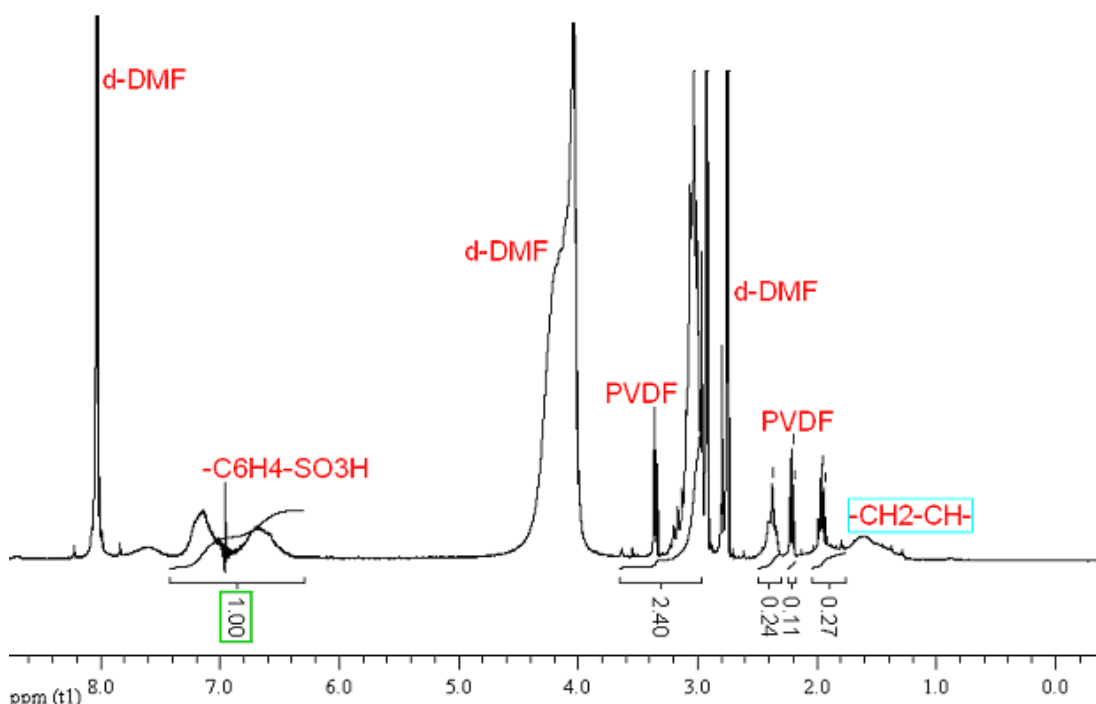


**Figure 4.22:**  $^1\text{H}$  NMR (d-DMF) Spectrum of PVDF-*g*-PSA Graft Copolymer

#### 4.2 Synthesis of PVDF-Based Graft Copolymers by AGET-ATRP

Copolymerisations of some monomers were also achieved via AGET-ATRP as described in experimental part. PGMA (PVDF-*g*-PGMA) graft PVPA (PVDF-*g*-PVPA), PAMPS (PVDF-*g*-PAMPS), PHEA (PVDF-*g*-PHEA) and PEGMAP (PVDF-*g*-PEGMAP) graft copolymers were not obtained. GMA, EGMAP, VPA, AMPS and HEA monomers were inappropriate for AGET-ATRP because of gelation during the polymerization process.

## 15. CONCLUSION

In the development of new proton exchange membranes (PEM) for fuel cells, functionalisation of a polymer offers many advantages, in particular with respect to the mechanical properties and the price of the material. Functionalisation is possible with graft or block copolymerization.

Flouro polymers, used in fuel cells, should present thermal stability as well as hydrolytic stability for fuel cell membrane operating conditions. The aim of this study was to synthesize graft copolymers, which possesses both properties.

Among many graft copolymerization techniques, in this study, atom transfer radical polymerization (ATRP) and activators generated by electron transfer (AGET) for ATRP was used in order to obtain PEMs. Many different monomers and synthesized functional group containing ionic monomers via hydrolysis reaction, grafted to the hydrophobic and chemically stable Poly(vinylidene fluoride) (PVDF) backbone in order to confer hydrophilic properties and consequently proton conductivity. In the graft copolymerization *tert*-butyl acrylate (*t*BA), 3-sulfo propyl methacrylate, potassium salt (SPMAP), 2-hydroxyl ethyl methacrylate (HEMA), 2-hydroxyl-ethyl acrylate (HEA), vinyl phosphoric acid (VPA), 2-acrylamido-2-methyl-1-propan sulphonic acid (AMPS), ethylene glycdyl methacrylate phosphate (EGMAP), glycdyl methacrylate (GMA), styrene (S) and synthesized monomers such as 3-sulfo propyl methacrylic acid three ethyleneamine salt (SAPMA-TEA) was used as monomers using PVDF-107 homopolymer as a macro-initiator in the presence of different catalyst complex and reaction conditions.

The PVDF-based graft copolymers were characterized using gel permeation chromatography (GPC) for determining the molecular weight shift, <sup>1</sup>H NMR (d-DMF) for compositions, Total Reflection Fourier Transform Infrared Spectroscopy (ATR FT-IR) for structure, differential scanning calorimetry (DSC) and thermo gravimetric analysis (TGA) for thermal properties.

The evaluation of the study reveals; only graft copolymers; PVDF-*g*-PAA, PVDF-*g*-PSPMAP, PVDF-*g*-PSAPMA-TEA, PVDF-*g*-PHEMA, PVDF-*g*-PSA were able

synthesize by ATRP. PGMA, PVPA, PAMPS and PHEA that might not co-operated with hydrophobic PVDF-107 macroinitiator. AMPS, VPA and also hydroxyl group containing HEA monomers gave polymeric gels during the ATRP polymerization method. Acidic group containing acrylic monomers AMPS and VPA have not yet been successfully polymerised by ATRP, because they can protonate ligands.

Many problems were encountered during the NMR and GPC characterization of PVDF-*g*-PSPMAP, PVDF-*g*-PSAPMA-TEA graft copolymers due to the insolubility in commercial solvents as tetrahydrofuran, chloroform and dimethylformamid.

The synthesized PVDF-*g*-PAA graft copolymer is inappropriate for fuel cell membrane applications because of its less hydrolytic stability and its decomposition starts at fuel cell working temperature.

Compared to PVDF-*g*-PAA and Nafion-117, PVDF-*g*-PSAPMA-TEA graft copolymer is dramatically more thermally stable at fuel cell working temperature. But the high solubility ratio of the PVDF-*g*-PSAPMA-TEA graft copolymer in water at 100 °C classifies it as inappropriate for fuel cell membrane in the operating conditions.

As an ATRP precursor, which possesses ionic moieties, HEMA with –OH functional group was grafted on to the PVDF backbone by ATRP. Compared to PVDF-*g*-PAA, PVDF-*g*-PSAPMA-TEA graft copolymers and Nafion-117 as a commercial product, PVDF-*g*-PHEMA graft copolymer is distinctively more thermally stable.

The detailed investigations on conductivity of PVDF-*g*-PSA graft copolymer is in progress.

## REFERENCES

- [1] Souzy, R., and Ameduri, B., 2005. Functional fluoropolymers for fuel cell membranes prog., *Polym. Sci.*, **30**, 644-687.
- [2] Ying, L., Wang, P., Kang, E. T., and Neoh, K.G., 2002. Synthesis and characterization of poly(acrylic acid)-graft-poly(vinylidene fluoride) copolymers and pH-sensitive membranes, *Macromolecules*, **35**, 673-679.
- [3] Scheirs, J., 1997. Modern Fluoropolymers, Scheirs J., Ed., John Wiley & Sons, New York, p. 3.
- [4] Gelin, M. P., and Ameduri, B., 2003. Synthesis of An Original Poly(vinylidene fluoride-co-hexafluoropropylene)-g-perfluoropolyether graft copolymer, *Journal of Fluorine Chemistry*, **119**, 53-58.
- [5] Sauguet, L., Boyer, C., Ameduri, B., and Boutevin, B., 2006. Synthesis and characterization of poly(acrylic acid)-graft-poly(styrene) graft copolymers obtained by atom transfer radical polymerization of styrene, *Macromolecules*, **39**, 9087-9101.
- [6] Hester, J. F., Banerjee, P., Won. T., Akthakul, A., Acar, M. H., and Mayes, A.M., 2002. ATRP of amphiphilic graft copolymers based on PVDF and their use as membrane additives, *Macromolecules*, **35**, 7652-7661.
- [7] Natanya, M., Hansen, L., Jankova, K., and Hvilsted S., 2002. AAc-g-PVDF Copolymer *Macromolecules*, **35**, 3.
- [8] Gelin, M. P., and Ameduri, B., 2008. *J Polym Sci Part B: Polym Phys*, **46**, 751
- [9] Inceoglu, S., Olugebefola, S. C., Acar, M. H. and Mayes, A. M., 2004. Atom transfer radical polymerization using poly(vinylidene fluoride) as macroinitiator, *Designed Monomers and Polymers*, **7**, 181.
- [10] Allcock, H. R., and Lampe, F., 1990 Contemporary Polymer Chemistry 2<sup>nd</sup> Ed., Prentice Hall, New Jersey.
- [11] Matyjaszewski, K., 1994. From living carbocationic to living radical polymerization, *J. Macromol. Sci. Pure Appl. Chem.* **A31**, 989.

- [12] **Matyjaszewski, K., and Sigwalt, P.,** 1994. Unified approach to living and nonliving cationic polymerization of alkenes, *Polymer Int.*, **35**, 1.
- [13] **Matyjaszewski, K. and Xia, J.,** 2001. Atom Transfer Radical Polymerization, *ACS, Chem Rev*, **101**, 2921–2990.
- [14] **Kato, M., Kamigaito, M., Sawamoto, M., and Higashimura T.,** 1995. Living cationic and radical polymerizations via reversible activation of carbon halogen bonds, *ACS*, 209:180-Poly. Part 2.
- [15] **Wang, J. S. and Matyjaszewski, K.,** 1995. Controlled living radical polymerization-halogen atom transfer radical polymerization promoted by a Cu(I)/Cu(II) redox process, *Macromolecules*, **28**, 7901–7910.
- [16] **Wang, J. S. and Matyjaszewski, K.,** 1995. Controlled living radical polymerization-ATRP in the presence of transition-metal complexes, *J. Am. Chem. Soc.*, **117**, 5614–5615.
- [17] **Davis, K.A. and Matyjaszewski, K.,** 2000. ATRP of tert-butyl acrylate and preparation of block copolymers, *Macromolecules*, **33**, 4039.
- [18] **Patten, T. E. and Matyjaszewski, K.,** 1998. ATRP and synthesis of polymeric materials, *Adv. Mater.*, **10**, 901.
- [19] **Matyjaszewski, K.,** 1999. Transition metal analysis in controlled radical polymerization: ATRP, *Chem. Eur. J.*, **5**, 3095.
- [20] **Patten, T. E. and Matyjaszewski, K.,** 1999. Cu(I) catalyzed ATRP, *Acc. Chem. Res.*, **32**, 895–903.
- [21] **Natanya, M., Hansen, L., Jankova, K., and Hvilsted S.,** 2007 Fluoropolymer materials and architectures prepared by controlled radical polymerizations, *E. Polym. J.*, **43**, 255-293.
- [22] **Xia, J. and Matyjaszewski, K.,** 1997. Controlled/"living" radical polymerization. Atom transfer radical polymerization using multidentate amine ligands, *Macromolecules*, **30**, 7697–7700.
- [23] **Xia, J. H. and Matyjaszewski, K.,** 1997. Controlled/"living" radical polymerization. Homogeneous reverse atom transfer radical polymerization using AIBN as the initiator, *Macromolecules*, **30**, 7692–7696.

- [24] **Wang, J. L., Grimaud, T. and Matyjaszewski, K.**, 1997. Kinetic study of the homogeneous atom transfer radical polymerization of methyl methacrylate, *Macromolecules*, **30**, 6507–6512.
- [25] **Matyjaszewski, K., and Davis, K. A.**, 2001. ABC triblock copolymers prepared using ATRP techniques, *Macromolecules*, **34**, 2101-2107.
- [26] **Xia, J., and Matyjaszewski, K.**, 1999. Homogeneous reverse ATRP of Styrene initiated by peroxides, *Macromolecules*, **32**, 2434–2437.
- [27] **Xia, J., Gaynor, S. G. and Matyjaszewski, K.**, 1998. Controlled/living radical polymerization. ATRP of acrylates at ambient temperature, *Macromolecules*, **31**, 5958–5959.
- [28] **Xia, J., Zang X., and Matyjaszewski, K.**, 2000. In transition metal macromolecular design; Boffa, L.S., Novak, B. M., Ed.; *ACS symposium series 760*; ACS Washington, DC, 207-223.
- [29] **Shipp, D. A., and Matyjaszewski, K.**, 2000. Kinetic analysis of controlled/"living" radical polymerizations by simulations. 2. apparent external orders of reactants in atom transfer radical polymerization, *Macromolecules*, **33**, 1553.
- [30] **Matyjaszewski, K.**, 1999. New copolymers by ATRP, *Macromolecular symposia*, **143**, 257.
- [31] **Matyjaszewski, K., and Miller, P.J.**, 1999. ATRP of methacrylates from dimethylsiloxane macroinitiators, *Macromolecules*, **32**, 8760.
- [32] **Matyjaszewski, K., and Jakubowski, W.**, 2005. Activator generated by electron transfer for atom transfer radical polymerization, *Macromolecules*, **38**, 4139.
- [33] **Min, K.** et al., 2005. Preparation of homopolymers and block copolymers in miniemulsion by ATRP using activators generated by electron transfer (AGET), *Journal of the ACS*, **127**, 3825.
- [34] **Hizal, G., Tunca, U., Aras, S., Mert, H.**, 2006. Air-stable and recoverable catalyst for the Atom Transfer Radical Polymerization of styrene; in situ generation of Cu(I) species via electron transfer reaction, *J. Polym. Sci. Part A Polym. Chem. Ed.*, **44**, 77-87.
- [35] **Matyjaszewski, K., Bombalski, L., Jakubowski, W., Min, K., Spanswick, J., and Tsarevsky, N.**, Int. Appl. (Carnegie Mellon University, USA), 96.

- [36] **Min, K., Jakubowski, W., and Matyjaszewski, K.**, 2006. AGET ATRP in the presence of air in miniemulsion and in bulk, *macromolecular rapid communications*, **27**, 594.
- [37] **K. Strasser**, 1992. *J. Power Sources*, **37**, 209.
- [38] **T. Norby**, 1999. *Solid State Ionics*, **97**, 1.
- [39] **M. Yamabe**, 1992. *Makromol. Chem. Macromol. Symp.* **64** , 11.
- [40] **Smart, B. E.**, 1995. Properties of fluorinated compounds, physical and physicochemical properties. In M. Hudlicky, S. E. Pavlathy Ed.), *Chemistry of organic fluorine compounds II ACS Monograph 197*, Washington DC, 997.
- [41] **Grot, W. G.**, 1984, of E. I. DuPont de Nemours and Company Wilmington, U. S. Patent, No:4443082.
- [42] **Beckerbauer, R.**, 1973, of E. I. DuPont de Nemours and Company Wilmington, U. S. Patent, No:3714245.
- [43] **Grot, W. G.**, 1973, of E. I. DuPont de Nemours and Company Wilmington, U. S. Patent, No:3718627.
- [44] **Kerres, J.**, 2001. *Membr. Sci*, **185**, 3.
- [45] **Queffelec, J., Gaynor, S. G., and Matyjaszewski, K.**, 2000. *Macromolecules*, **33**, 8629.
- [46] **Zukowska, G., Williams, J., Stevens, J.R., Jeffery, K.K., Lewera, A., Kulesza, P.J.**, 2004. The application of acrylic monomers with acidic groups to synthesis of proton conducting polymer gels, *Solid State Ionics*, **167**, 123-130.
- [47] **Samms, R., Wasmus, S., Savinell, R.F.**, 1996. Thermal stability of Nafion® in simulated fuel cell environments, *J.Electrochem.Soc*, **143**, 5.
- [48] **Kang, E.T., Ying, L., Wang, P., and Neoh, K.G.**, 2002. Synthesis and characterization of Poly (acrylic acid)-graft-poly(vinylidene fluoride) copolymers as pH-sensitive membranes, *Macromolecules*, **35**, 673-679.
- [49] **Hickner, M.A., Ghassemi, H., Kim, Y.S., Einsla B.R., and McGrath, J.E.** 2004. Alternative polymer systems for proton exchange membranes (PEMS), *Chem. Rev.*, **104**, 4587-4612.

- [50] **Grillone, A.M., Panero, S., Retamal, B.A., and Scrosati, B.**, 1999. Proton polymeric gel electrolyte membranes based on polymethylmethacrylate, *J. Electrochem. Soc.*, **146**, 27.

## **AUTOBIOGRAPHY**

Born in 1980 in Hannover, Germany, she graduated from Ugur High School and attended the Chemistry Department of Istanbul Technical University in 2000. After graduating from Istanbul Technical University in 2006, she was registered as a M.Sc. student to Istanbul Technical University, Polymer Science and Technology Department of the Institute of Science and Technology in the same year. Her master thesis was supported by I.T.U. Between 2006-2008 she worked as a research assistant at the TUBİTAK-104M409 project in Istanbul Technical University.